Cell cycle dependent association of polo kinase Cdc5 with CENP-A contributes to faithful chromosome segregation in budding yeast

Prashant K. Mishra[a], Gudjon Olafsson[b], Lars Boeckmann[a,e], Timothy J. Westlake[a], Ziad M. Jowhar[a], Lauren E. Dittman[a], Richard E. Baker[c], Damien D'Amours[d], Peter H. Thorpe[b], and Munira A. Basrai[a*]

[a]Genetics Branch, National Cancer Institute, National Institutes of Health, Bethesda, MD, USA; [b]Queen Mary University of London, UK; [c]University of Massachusetts Medical School, Worcester, MA, USA; [d]University of Ottawa, Ontario, Canada.

[e]Present address: University Medical Center, Rostock, Germany.

[*]**Address correspondence to:** Munira A. Basrai (Email: basraim@nih.gov)

ABSTRACT

Evolutionarily conserved polo-like kinase, Cdc5 (Plk1 in humans) associates with kinetochores during mitosis, however, the role of cell cycle dependent centromeric (*CEN*) association of Cdc5 and its substrates that exclusively localize to the kinetochore have not been characterized. Here we report that evolutionarily conserved *CEN* histone H3 variant, Cse4 (CENP-A in humans) is a substrate of Cdc5, and that the cell cycle regulated association of Cse4 with Cdc5 is required for cell growth. Cdc5 contributes to Cse4 phosphorylation *in vivo* and interacts with Cse4 in mitotic cells. Mass spectrometry analysis of *in vitro* kinase assays showed that Cdc5 phosphorylates nine serine residues clustered within the N-terminus of Cse4. Strains with *cse4-9SA* exhibit increased errors in chromosome segregation, reduced levels of *CEN*-associated Mif2 and Mcd1/Scc1 when combined with a deletion of *MCM21*. Moreover, the loss of Cdc5 from the *CEN* chromatin contributes to defects in kinetochore integrity and reduction in *CEN*-associated Cse4. The cell cycle regulated association of Cdc5 with Cse4 is essential for cell viability as constitutive association of Cdc5 with Cse4 at the kinetochore leads to growth defects. In summary, our results have defined a role for Cdc5-mediated Cse4 phosphorylation in faithful chromosome segregation.

Abbreviations used:

CEN, centromere;

CAR, cohesin-associated region;

CATD, centromere targeting domain;

CF, chromosome fragment;

ChIP, chromatin immunoprecipitation;

FACS, fluorescence activated cell sorting;

FEAR, Cdc fourteen early anaphase release;

FOA, 5-fluoroorotic acid;

HFD, histone fold domain;

IP, immunoprecipitation;

GBP, GFP-binding protein;

GFP, green fluorescent protein;

LC-MS/MS, liquid chromatography-tandem mass spectrometry;

PBD, polo-box domain;

PTM, post-translational modification;

qPCR, quantitative PCR;

RFP, red fluorescent protein;

SPA, selective ploidy ablation;

SPI, synthetic physical interaction;

YFP, yellow fluorescent protein.

INTRODUCTION

Faithful chromosome segregation is essential for the growth and cellular proliferation of organisms because defects in this process results in aneuploidy, which has been observed in human diseases such as cancer, and developmental disorders (Santaguida and Amon, 2015). A key determinant for high fidelity chromosome segregation is the kinetochore, which is composed of centromeric (*CEN*) DNA, associated proteins and a unique chromatin structure (Verdaasdonk and Bloom, 2011; Burrack and Berman, 2012; Musacchio and Desai, 2017). *CENs* in budding yeast are composed of ~125 bp of unique DNA sequence (Clarke and Carbon, 1980), whereas *CENs* in other eukaryotes are several mega-base pairs of DNA representing sequence repeats, species-specific satellite arrays, or retrotransposon-derived sequences (Verdaasdonk and Bloom, 2011). Despite the *CEN* sequence divergence, the role of *CEN* in chromosome segregation is evolutionarily conserved (Verdaasdonk and Bloom, 2011; Burrack and Berman, 2012). Moreover, many of the ~70 kinetochores proteins representing different sub-complexes from budding yeast (Westermann *et al.*, 2003; Cho *et al.*, 2010; Biggins, 2013) are functionally conserved (Musacchio and Desai, 2017). For example, *CEN* identity in eukaryotic organisms is specified by an epigenetic mark in the form of specialized nucleosomes containing Cse4 (CENP-A in humans, Cid in flies, Cnp1 in fission yeast) (Sullivan *et al.*, 1994; Stoler *et al.*, 1995; Meluh *et al.*, 1998; Henikoff *et al.*, 2000; Takahashi *et al.*, 2000). In budding yeast, Cse4 contains two distinct domains. The evolutionarily conserved C-terminus histone fold domain (HFD) carries a centromere targeting domain (CATD), which is essential for recruitment and incorporation of Cse4 into the *CEN* chromatin (Meluh *et al.*, 1998; Keith *et al.*, 1999). The N-terminus of Cse4 (~129 amino

acids) interacts with kinetochore proteins such as the components of the COMA complex (Ctf19, Okp1, Mcm21, and Ame1), and facilitates their recruitment to the *CEN* (Ortiz *et al.*, 1999). Moreover, the N-terminus of CENP-A also directs the targeting of other kinetochore proteins to the *CEN* (Van Hooser *et al.*, 2001). In addition, post-translational modifications (PTMs) of Cse4, namely, phosphorylation, ubiquitination, sumoylation, methylation, and acetylation also regulate faithful chromosome segregation (Hewawasam *et al.*, 2010; Ranjitkar *et al.*, 2010; Samel *et al.*, 2012; Au *et al.*, 2013; Boeckmann *et al.*, 2013; Ohkuni *et al.*, 2016; Hoffmann *et al.*, 2018). Previous studies have shown that an evolutionarily conserved Ipl1/Aurora B contributes to phosphorylation of Cse4 (Buvelot *et al.*, 2003; Boeckmann *et al.*, 2013). Using mass spectrometric analysis of Cse4 from wild-type yeast cells, we have previously reported the *in vivo* phosphorylation of Cse4 sites S22, S33, S40, and S105 (Boeckmann *et al.*, 2013). Moreover, a recent study has confirmed the presence of *in vivo* phosphorylation of Cse4 on serine 33, and shown that *cse4-S33A* mutants show reduced levels of Cse4 at *CEN* when combined with the mutations in histone H2A and H4 (Hoffmann *et al.*, 2018). However, the protein kinase responsible for this modification has not been defined.

Evolutionarily conserved polo-like kinase Cdc5 (Plk1 in humans) regulates several aspects of mitotic cell cycle and chromosome segregation (St-Pierre *et al.*, 2009; Walters *et al.*, 2014; Zitouni *et al.*, 2014) including sister chromatid separation by phosphorylation of Mcd1/Scc1 promoting its proteolytic cleavage by separase (Uhlmann *et al.*, 2000; Alexandru *et al.*, 2001). Cdc5 associates with *CEN* and cohesin-associated regions (*CAR*s) along chromosome arms in a cell cycle regulated manner and is required

for the removal of cohesins from the *CEN* chromatin during mitosis (Rossio *et al.*, 2010; Mishra *et al.*, 2016). In addition to cohesins Mcd1/Scc1, and Smc3, several other Cdc5-interacting proteins have been identified, such as protein kinase Swe1, protein phosphatase Cdc14, spindle pole body components Spc72 and Spc110, and the Cdc *F*ourteen *E*arly *A*naphase *R*elease (FEAR) network protein Slk19 (Alexandru *et al.*, 2001; Snead *et al.*, 2007; Park *et al.*, 2008; Rahal and Amon, 2008; Roccuzzo *et al.*, 2015; Botchkarev and Haber, 2018). Moreover, Plk1 in human cells has been shown to phosphorylate kinetochore protein Mis18BP1 to facilitate the assembly of newly synthesized CENP-A at the *CEN* (McKinley and Cheeseman, 2014), however, a homolog of Mis18BP1 has not been identified in budding yeast. Intriguingly, a candidate-based screen using Cdc5 polo-box domain (PBD) as a bait showed an enrichment of kinetochore proteins Cse4 and Tid3 (Snead *et al.*, 2007), however, the molecular significance of the interaction of Cdc5 with Cse4, and Cdc5 substrates that localize exclusively to the kinetochore have not been characterized.

In this study, we show that Cdc5 interacts *in vivo* with Cse4 in mitotic cells (G2/M), and phosphorylates Cse4 *in vitro* and *in vivo*. Cdc5-mediated Cse4 phosphorylation regulates faithful chromosome segregation as evident from the increased frequency of chromosome loss in the non-phosphorylatable *cse4* mutant (*cse4-9SA)* when combined with a deletion of *MCM21*. Significant reduction in levels of kinetochore protein Mif2, and cohesin Mcd1/Scc1 are observed at *CEN* chromatin in a *cse4-9SA mcm21Δ* strain. The constitutive association of Cdc5 with Cse4 at the kinetochore causes growth defects suggesting that cell cycle regulated interaction of these two proteins restricted to mitosis

is essential for cell viability. In summary, we have identified Cse4 as a substrate for Cdc5, and shown that Cdc5 mediated phosphorylation of Cse4 contributes to high fidelity chromosome segregation.

RESULTS

Cdc5 interacts with Cse4 *in vivo* in a cell cycle dependent manner

The budding yeast polo-like kinase, Cdc5 associates with centromeres in mitosis and facilitates the removal of *CEN* cohesin (Mishra *et al.*, 2016). Cse4 was enriched in a screen to identify proteins that interact with the polo-box domain (PBD) of Cdc5 used as a bait (Snead *et al.*, 2007). We explored the role of the interaction of Cdc5 with Cse4 in faithful chromosome segregation. Immunoprecipitation (IP) experiments were done to determine if Cdc5 interacts with Cse4 *in vivo*. We constructed a strain that expresses HA-tagged Cdc5, and Flag-tagged Cse4. IP was done using protein extracts from logarithmically growing asynchronous cultures (Figure 1A and B). Western blotting showed that Cdc5 interacts with Cse4 *in vivo*, whereas no signals were detected in a control experiment using an untagged strain (Figure 1C).

To determine whether the *in vivo* interaction of Cdc5 with Cse4 is cell cycle regulated, IP experiments were performed using cells synchronized in G1 (α-factor treatment), S (hydroxyurea treatment), or G2/M (nocodazole treatment) stages of the cell cycle. The cell cycle synchronization was confirmed by FACS (Figure 1A), and examination of nuclear and cell morphology (Figure 1B). In agreement with previous studies (Charles *et al.*, 1998; Mishra *et al.*, 2016), Cdc5 was expressed in S, and G2/M phases of the cell

cycle, whereas no protein expression was detected in G1 cells (Figure 1C). IP results showed an *in vivo* interaction between Cdc5 and Cse4 in G2/M cells (Figure 1C). No interaction of Cdc5 with Cse4 was detected in G1 and S-phase cells despite the expression of Cdc5 in S-phase (Figure 1C). As expected, no signals were detected in control experiments performed with an untagged strain (Figure 1C). Taken together, these results provide evidence for cell cycle regulated *in vivo* interaction of Cdc5 and Cse4 that occurs in mitotic cells.

Cdc5 phosphorylates Cse4 *in vitro*

To determine whether Cdc5 phosphorylates Cse4 directly, we performed *in vitro* kinase assays with radiolabeled ATP using Cdc5 purified from yeast (Ratsima *et al.*, 2011), and Cse4 purified from *Escherichia coli*. Cse4 was radiolabeled in the presence of Cdc5, whereas no signal was observed from control *in vitro* assays containing purified histone H3 (Figure 2A). We next performed *in vitro* kinase assay by incubating purified Cse4 either with wild type Cdc5 or its kinase inactive Cdc5kd protein [i.e., Cdc5-K110M; (Ratsima *et al.*, 2011)]. Radiolabeled Cse4 was detected in the presence of wild-type Cdc5 but not the kinase inactive *cdc5kd* protein (Figure 2B) suggesting that the assay specifically reflects Cdc5 mediated kinase activity towards Cse4.

Cdc5 mediated phosphorylation of Cse4 occurs largely within the N-terminus of Cse4

To identify Cse4 residues phosphorylated by Cdc5, we performed an *in vitro* kinase assay as described in Figure 2A, and samples were analyzed by liquid chromatography-tandem

mass spectrometry (LC-MS/MS). A total of nine phosphorylated serine sites (S9, S10, S14, S16, S17, S33, S40, S105, and S154) were identified (Figure 3A). Except for S154, which is located within the C-terminus histone fold domain, the remaining eight serine residues are largely clustered within the N-terminus of Cse4. Sequence analysis showed that these sites are evolutionarily conserved among different yeast species containing point centromeres (Figure 3B). To explore the physiological effects of the Cdc5 mediated Cse4 phosphorylation, we constructed a phosphorylation deficient *cse4* mutant, in which all nine phosphorylated serines were changed to alanine (*cse4-9SA*). We examined the ability of *cse4-9SA* to complement the growth of *cse4Δ* strain using 5-fluoroorotic acid (5-FOA) mediated plasmid shuffle assay (Widlund and Davis, 2005; Tukenmez *et al.*, 2016). Strains carrying *cse4-9SA* grew robustly on 5-FOA plates confirming that *cse4-9SA* allele can complement the *cse4*Δ (Figure 3C). As expected, no growth on 5-FOA was observed in *cse4*Δ strains with vector used as a negative control (Figure 3C). We next examined the levels of endogenously HA-tagged Cse4 and Cse4-9SA at the *CEN* in a wild type strain grown at 25°C. ChIP-qPCR showed that the *CEN* levels of Cse4 and Cse4-9SA were not significantly different (Figure 3D, *p*-value = >0.05). No significant enrichment of Cse4 or Cse4-9SA was detected at a negative control non-*CEN HML* locus (Figure 3D).

Cdc5 contributes to the phosphorylation of Cse4 *in vivo*

We have previously used a α-rabbit polyclonal phospho-Cse4 specific (αp-Cse4) antibodies that did not react with Cse4-4SA in which four serine sites of Cse4 were mutated to alanine (S22A, S33A, S40A, and S105A) to show increased levels of

phosphorylated Cse4 at the *CEN* (Boeckmann *et al.*, 2013). Among the four serine sites, three (S33, S40 and S105) are phosphorylated by Cdc5 *in vitro* (Figure 3A). Hence, we used αp-Cse4 antibody to investigate the role of Cdc5 in Cse4 phosphorylation *in vivo*. Western blot analysis of affinity-purified Cse4 showed strong reactivity to αp-Cse4 but no signals were detected with Cse4-9SA suggesting that the nine serine residues in Cse4 contribute to the reactivity of Cse4 with αp-Cse4 antibody (Figure 3E). Since we observed an *in vivo* interaction of Cse4 and Cdc5 in metaphase (Figure 1), we used the αp-Cse4 antibody to examine the *in vivo* levels of Cse4 phosphorylation in metaphase cells from wild type and a well-characterized temperature-sensitive *cdc5-99* mutant (St-Pierre *et al.*, 2009). Western blot analysis was done using affinity purified Cse4 from metaphase cells collected ~110 min after release from G1 arrest into pheromone-free media at 25° and 37°C (Figure 3F and G). Our results showed similar levels of expression of Cse4 in wild type and *cdc5-99*, both at permissive (25°C) and non-permissive (37°C) temperature of growth (Figure 3H). The levels of p-Cse4 were similar at 25°C between wild type and *cdc5-99*; however, the levels of p-Cse4 were lower in *cdc5-99* than the wild type strain at 37°C (Figure 3H). We quantified the fraction of phosphorylated Cse4, and normalized this to the total Cse4 levels for each sample. The level of phosphorylated Cse4 was significantly lower (~30 %) in *cdc5-99* than the wild type strain at 37°C (Figure 3I). Taken together, these results indicate that Cdc5 contributes to the phosphorylation of Cse4 *in vivo*.

Cse4 phosphorylation deficient and *mcm21Δ* mutants exhibit synthetic defects in chromosome segregation fidelity

With the exception of one serine, eight of the nine Cse4 serine residues that are phosphorylated by Cdc5 are in the N-terminus of Cse4 (Figure 3A). Cse4 interacts *in vivo* with Ctf19 and Mcm21 (Ortiz *et al.*, 1999; Ranjitkar *et al.*, 2010), and this interaction is mediated by the N-terminus of Cse4 (Chen *et al.*, 2000). Genetic interactions have also been reported for mutants of *cse4* with *ctf19*Δ and *mcm21*Δ (Samel *et al.*, 2012). Moreover, Mcm21 and Ctf19 have additional roles in maintenance of *CEN* cohesion (Ng *et al.*, 2009; Hinshaw *et al.*, 2017), a biological process in which Cdc5 is also involved (Rossio *et al.*, 2010; Mishra *et al.*, 2016). Since the Cdc5 target sites in Cse4 are clustered largely within the N-terminus of Cse4, we assayed chromosome segregation in *cse4-9SA* strains in combination with deletions of *MCM21* or *CTF19*. The loss of a non-essential reporter chromosome fragment (CF) was measured using the colony color assay as described previously (Spencer *et al.*, 1990). The frequency of CF loss is slightly higher in *cse4-9SA* when compared to the wild type strain, but the difference is not statistically significant (Figure 4A). The frequency of CF loss in *mcm21Δ* and *ctf19Δ* is significantly higher than the wild type or *cse4-9SA* strains (Figure 4A). The frequency of CF loss in *ctf19Δ* and *cse4-9SA ctf19Δ* mutant is largely similar and does not differ significantly from each other (*p*-value = 0.3). However, the frequency of CF loss in *cse4-9SA mcm21Δ* mutant is significantly higher than the *mcm21Δ* (~5-fold; *p*-value = 0.0023), *cse4-9SA* (~30-fold; *p*-value = 0.0009), and the wild type (~50-fold; *p*-value = 0.0008) strains (Figure 4A). These results show that Ctf19 independent events contribute to increased chromosome loss in *cse4-9SA mcm21Δ* strains but do not rule out a role for Cse4-9SA in the loading of Ctf19 to the centromeric chromatin.

We next examined if defects in phosphorylation of Cse4-S33 affects chromosome segregation when combined with *mcm21*Δ. The rationale for this experiment is based on our identification of Cse4-S33 as a potential Cdc5 phosphorylation site and recent studies showing that phosphorylation deficient *cse4-S33A* and mutations in histones H2A and H4 exhibit synthetic defects in *CEN* deposition of Cse4 (Hoffmann *et al.*, 2018). The frequency of CF loss in *cse4-S33A* is statistically similar to that observed for wild type or *cse4-9SA* strains (*p*-value = 0.85). However, the frequency of CF loss in *cse4-S33A mcm21Δ* mutant is significantly higher than the *mcm21Δ* (~2-fold; *p*-value = 0.021), but is significantly lower than *cse4-9SA mcm21Δ* (*p*-value= 0.0094) strains (Figure 4A). Taken together, these results support a role for phosphorylation of Cse4 in faithful chromosome segregation.

Phosphorylation of Cse4 regulates the *CEN* association of kinetochore protein Mif2, and cohesin component Mcd1/Scc1

Our results for increased chromosome loss in *cse4-9SA mcm21Δ* strains prompted us to examine the role of Cse4 phosphorylation in kinetochore structure. Hence, we examined the levels of *CEN*-associated kinetochore protein Mif2, the yeast ortholog of mammalian CENP-C, which contributes to localization of Cse4 at the *CEN*, maintenance of spindle integrity, and cohesin-based partitioning mechanisms at the kinetochore (Brown *et al.*, 1993; Meluh and Koshland, 1995; Cohen *et al.*, 2008; Ho *et al.*, 2014; Tsabar *et al.*, 2016). ChIP experiments were performed to determine the enrichment of Mif2 at *CEN*, and *CARs*: peri-*CEN* (134), chromosomal arm (261), and negative control region (310) on chromosome III in cells synchronized with nocodazole in the G2/M stage of the cell

cycle (Figure 4B). No significant enrichment of Mif2 was detected at *CARs* located at peri-*CEN* (134), chromosomal arm (261) or a negative control region (310) (Figure 4C). ChIP-qPCR revealed mildly lower levels of *CEN*-associated Mif2 in *cse4-9SA* than the wild type strain (Figure 4C). However, Mif2 levels at *CEN* were significantly lower in *cse4-9SA mcm21Δ* than the wild type or single mutant strains (Figure 4C). Western blotting revealed that the reduction in *CEN*-associated Mif2 in the *cse4-9SA mcm21Δ* strain was not due to reduction in the levels of Mif2 (Figure 4D). Based on these results, we conclude that phosphorylation of Cse4 regulates *CEN* association of Mif2 in the absence of Mcm21.

Previous studies have shown that *cse4* and *mcm21Δ* strains exhibit reduced levels of cohesin at the *CEN* and peri-*CEN* chromatin (Weber *et al.*, 2004; Ng *et al.*, 2009). Deletion of *MCM21* results in the failure of Ctf19 loading onto *de novo* kinetochores suggesting that Mcm21 is required for the assembly or productive association of Ctf19 complex at the kinetochores (Lang *et al.*, 2018). Moreover, defects in levels of *CEN* cohesin have been linked with altered kinetochore function (Brooker and Berkowitz, 2014). Notably, Cdc5 regulates the removal of *CEN* cohesin (Alexandru *et al.*, 2001; Mishra *et al.*, 2016). Based on these results, we postulated that defects in Cdc5 mediated phosphorylation of Cse4 may affect *CEN* association of cohesins in an *mcm21Δ* strain. ChIP experiments were performed to examine the enrichment of cohesin component Mcd1/Scc1 at *CEN*, and *CARs* in mitotic cells. Mcd1/Scc1 enrichment at chromosomal arm region (261) was largely similar, and was not significantly different among the strains. No significant enrichment of Mcd1/Scc1 was detected at a negative control

region (310; Figure 4E). Enrichment of Mcd1/Scc1 at *CEN*, and *CARs* located at peri-*CEN* (134) and chromosomal arm (261) was observed in wild type, and *cse4-9SA* strains (Figure 4E). Significantly reduced levels of Mcd1/Scc1 were observed at *CEN*, and peri-*CEN* (134) in a *mcm21Δ* strain (Figure 4E), and this reduction was further exacerbated in *cse4-9SA mcm21Δ* strain in comparison to wild type, *cse4-9SA,* or *mcm21Δ* strains (Figure 4E). Reduction in enrichment of Mcd1/Scc1 at *CEN* and peri-*CEN* in *cse4-9SA mcm21Δ* strain was not due to reduction in the protein expression of Mcd1/Scc1 (Figure 4F). Based on these results, we conclude that phosphorylation of Cse4 affects the *CEN* association of Mif2 and cohesins during mitosis.

Centromeric association of Cdc5 regulates *CEN*-associated Cse4 and structural integrity of kinetochores

Cdc5 associates with *CEN* chromatin during mitosis (Mishra *et al.*, 2016), which correlates with the increased levels of phosphorylated Cse4 at the *CEN* (Boeckmann *et al.*, 2013). Based on these results, we posit that the absence of Cdc5 from the *CEN* chromatin may exhibit alterations in levels of *CEN* associated Cse4, and defects in structural integrity of kinetochores. To address this hypothesis, we assayed the *CEN* association of Cdc5, and Cdc5-99 mutant grown at permissive (25°C) and non-permissive (37°C) temperatures (St-Pierre *et al.*, 2009). Western blot analysis showed similar levels of expression of Cdc5 and Cdc5-99 at the permissive temperature of 25°C and after a shift to the non-permissive temperature of 37°C (Figure 5A). ChIP-qPCR showed that the enrichment of Cdc5 and Cdc5-99 at *CEN* chromatin (*CEN1, CEN3,* and *CEN5*) is not significantly different at 25°C (*p*-value = >0.05). However, reduced levels

of Cdc5-99 were observed at *CEN* chromatin (~5-9 fold) at 37°C (Figure 5B). There was no significant enrichment of Cdc5 or Cdc5-99 at non-*CEN* negative control region (6K120) relative to that observed at the *CEN3* (Figure 5B). Overall, these results show that mutant Cdc5-99 cannot associate with *CEN* at the non-permissive temperature.

We next examined the effect of loss of *CEN* association of Cdc5-99 on the levels of endogenously HA-tagged Cse4 at the *CEN* using wild type and *cdc5-99* strains grown at 25°C and after a shift to 37°C. ChIP-qPCR showed that the levels of *CEN* associated Cse4 in wild type and *cdc5-99* strains at 25°C are not statistically different (*p*-value = >0.05). However, enrichment of Cse4 at the *CEN* was reduced significantly in *cdc5-99* (1.29% of input at *CEN1*, 1.33% at *CEN3*, and 1.31% at *CEN5*) compared with the levels observed in a wild type strain (2.49% at *CEN1*, 2.26% at *CEN3*, and 2.42% at *CEN5*) at 37°C (Figure 5C). No significant enrichment of Cse4 was detected at the non-*CEN HML* locus used as a negative control (Figure 5C).

We reasoned that the reduced levels of *CEN* associated Cse4 in *cdc5-99* strain at 37°C (Figure 5C) may affect the structural integrity of kinetochores. Hence, we used *DraI* restriction enzyme accessibility assay as described previously to measure the structural integrity of the kinetochore (Saunders *et al.*, 1990; Mishra *et al.*, 2013). DNA was extracted from nuclei prepared from wild type and *cdc5-99* strains grown at 25°C and 37°C after treatment with 100 U/mL *DraI*. We quantified the levels of *DraI* accessibility by qPCR using primers flanking *CEN3* or a non-*CEN* control *ADP1* region (Mishra *et al.*, 2013). The *CEN3* chromatin in *cdc5-99* strain was significantly more susceptible to *DraI*

digestion (~2-fold) at 37°C than that observed at 25°C (Figure 5D). No significant increased *DraI* accessibility of *CEN3* chromatin was observed in a wild type strain at 25°C or 37°C (~1.1-1.8%), which was largely similar to that observed for *cdc5-99* strain at 25°C (~1.4-1.9%) (Figure 5D). The *ADP1* chromatin showed low sensitivity to *DraI* treatments (~1.0-1.3%), and no significant differences in the accessibility of *DraI* to *ADP1* region were observed between wild type and *cdc5-99* strains grown at 25° or 37°C (Figure 5D). These results show that *CEN* association of Cdc5 regulates structural integrity of kinetochores.

Cell cycle regulated interaction of Cdc5 with Cse4 is required for cell growth

In vivo interaction between Cdc5 and Cse4 is detectable only in mitotic cells (G2/M; Figure 1C). Hence, we sought to understand the physiological significance of cell cycle dependent association of Cdc5 with Cse4. We postulated that constitutive association of Cdc5 with Cse4 throughout the cell cycle may affect cell growth. Hence, we used the synthetic physical interaction (SPI) assay (Olafsson and Thorpe, 2015) to examine the effect of constitutive association of Cdc5 with Cse4 at kinetochores. Wild type Cdc5 protein was linked to the sequence encoding a GFP-binding protein (GBP) (Rothbauer *et al.*, 2008), which also carries a tag representing red fluorescent protein (RFP). Plasmids expressing Cdc5-GBP, or control-GBP (vector carrying GBP domain) were transformed into strains carrying Cse4-GFP, Cep3-GFP or non-GFP controls. Microscopic examinations of cells confirmed the colocalization of Cdc5 with Cse4-GFP or Cep3-GFP (Figure 6A and B). Cep3 is an essential kinetochore protein that binds *CDEIII* region of the *CEN* (Lechner and Carbon, 1991; Strunnikov *et al.*, 1995), and is about 44 nm away

from Cse4 at the metaphase kinetochores (Haase *et al.*, 2013). In control experiment with GBP-RFP, only one or two-foci of Cse4 were observed in a cell, however constitutive association of Cdc5 with Cse4 causes alteration in its localization pattern as evident from the multiple and diffused Cse4 foci (Figure 6A). Constitutive association of Cdc5 with inner kinetochore protein Cep3, which was used as a control, does not exhibit altered localization phenotype (Figure 6B).

We next performed growth assays using selective ploidy ablation (SPA) technology (Reid *et al.*, 2011) with 16 replicates per strain to examine the effect of constitutive association of Cdc5 on Cse4. Plates were scanned, and growth measurements were determined using the ScreenMill software (Dittmar *et al.*, 2010). Colony sizes were quantified and compared among strains as described previously (Olafsson and Thorpe, 2015). We observed that constitutive association of Cdc5 with Cse4-GFP causes growth defects, whereas no growth inhibition was observed with inner kinetochore protein, Cep3-GFP or non-GFP control strains (Figure 6C and D). The growth defects were mediated by the kinase activity of Cdc5 because strains expressing kinase inactive *cdc5kd* exhibited growth phenotypes similar to Cep3-GFP or non-GFP control strains (Figure 6C and D). To determine whether constitutive association of Cdc5 with Cse4 causes arrest at a particular cell cycle stage, we created conditionally-expressed Cdc5 in which the polo box domain was replaced with GBP (*Cdc5ΔC-GBP*) and its kinase inactive mutant (*cdc5ΔCkd-GBP*) under the control of *GAL1* promoter. Cdc5ΔC-GBP was used because overexpression of full length Cdc5 is lethal. *GALCdc5ΔC-GBP* and *GALcdc5ΔCkd-GBP* were expressed in a wild type and Cse4-YFP strains. Consistent with the results of the SPI assay, constitutive expression of *Cdc5ΔC-GBP* causes lethality in Cse4-YFP strain,

but not in a wild type strain (Figure 6E). Hence, we assayed the cell cycle stages of *GALCdc5ΔC-GBP* in Cse4-YFP strain after 4 hours of growth on galactose. The cell cycle stages categorized based on nuclear position and cell morphology showed that constitutive association of Cdc5 with Cse4 does not cause accumulation of cells in any specific cell cycle stage (Figure 6F). The cell cycle distribution of strains expressing *GALCdc5ΔC-GBP* is not statistically different from *GALcdc5ΔCkd-GBP* or an empty vector control (Figure 6F). To further determine the biological significance of constitutive phosphorylation of Cse4, we constructed the phospho-mimetic *cse4* mutant, in which all nine phosphorylated serines were changed to aspartic acid (*cse4-9SD*), and examined its ability to complement the growth of a *cse4Δ* strain after loss of *CSE4/URA3* plasmid by counterselection on medium containing 5-FOA. Strains with Cse4 and *cse4-9SA* grew robustly on plates containing 5-FOA, whereas strains carrying *cse4-9SD* did not exhibit growth on 5-FOA plates after 6 days of incubation at 25°C (Figure 6G). Taken together, these results show that constitutive association of Cdc5 with Cse4 is detrimental to cell growth and define a physiological role for cell cycle regulated association of Cdc5 with Cse4.

DISCUSSION

Polo-like kinase Cdc5 and its homologs regulate different stages of the mitotic and meiotic cell cycle, and high-fidelity chromosome segregation (Zitouni *et al.*, 2014). Cdc5 in budding yeast associates with the *CEN* chromatin during mitosis (Mishra *et al.*, 2016), however kinetochore specific substrates for Cdc5, and the physiological role of Cdc5-mediated phosphorylation of kinetochore proteins have not been characterized. In this

study, we have identified Cdc5 as a kinase for Cse4 and defined a role for Cdc5-mediated Cse4 phosphorylation in faithful chromosome segregation. Our results have shown that: (1) Cdc5 interacts *in vivo* with Cse4 in mitotic cells, (2) Cdc5 phosphorylates Cse4 *in vitro*, (3) Cdc5 contributes to phosphorylation of Cse4 *in vivo*, (4) mutations that abrogate Cdc5-mediated phosphorylation of Cse4 (*cse4-9SA*) lead to increased chromosome loss, reduction in kinetochore protein Mif2, and cohesin Mcd1/Scc1 at the *CEN* chromatin, (5) constitutive association of Cdc5 with Cse4 at the kinetochore causes growth defects, and (6) mutations that mimic phosphorylation (*cse4-9SD*) lead to loss of viability. We propose that the cell cycle regulated association of Cdc5 with Cse4 regulates phosphorylation of Cse4 for the structure and function of the kinetochore and cell viability.

In vitro assay showed that the kinase domain of Cdc5 mediates the phosphorylation of Cse4. The failure of Cdc5 to phosphorylate histone H3 implies that *in vitro* phosphorylation observed is specific to Cse4. Mass spectrometric analysis revealed that nine of the eight serine residues in Cse4 phosphorylated by Cdc5 are within the N-terminus domain of Cse4 (S9, S10, S14, S16, S17, S33, S40, S105). We previously showed *in vivo* phosphorylation of Cse4 serine sites: S22, S33, S40, and S105 using mass spectrometric analysis of Cse4 from wild-type yeast cells. The phosphorylation of S40 and S105 is regulated by Aurora B kinase Ipl1 *in vitro* (Boeckmann *et al.*, 2013). Phosphorylation of Cse4 site S33 has been linked with its *CEN* deposition as reduced levels of Cse4 were detected in histone H2A and H4 mutants with phosphorylation deficient *cse4-S33A* (Hoffmann *et al.*, 2018), however the kinase responsible for this

phosphorylation has not been identified. Our *in vitro* kinase assay revealed that S33 of Cse4 is a target site for Cdc5 phosphorylation. Moreover, biochemical assays showed that Cdc5 contributes to the phosphorylation of Cse4 *in vivo*. For example, using αp-Cse4 antibody, we observed a reduction in phosphorylated Cse4 in metaphase cells of a temperature-sensitive *cdc5-99* mutant (St-Pierre *et al.*, 2009). It is notable that a fraction of Cse4 can still be phosphorylated in *cdc5-99* mutant suggesting that this may be mediated by the Ipl1 kinase as reported previously (Boeckmann *et al.*, 2013). Together, these data show that phosphorylation of Cse4 is facilitated by at least these two kinases. It is possible that Cdc5 and Ipl1 may regulate differential phosphorylation of Cse4 in response to geometric or conformational changes at the kinetochores during the cell cycle (Pearson *et al.*, 2004; Yeh *et al.*, 2008; Verdaasdonk *et al.*, 2012). This conclusion is consistent with previous reports for multiple protein kinases coordinatively modifying a substrate in response to cell cycle dynamics. For example, Cdc28 and Cdc5 work synergistically for the phosphorylation of Swe1 and condensin in budding yeast (Asano *et al.*, 2005; St-Pierre *et al.*, 2009; Robellet *et al.*, 2015). Moreover, cyclin-dependent kinase (Cdk), meiosis-specific kinase (Ime2), and Cdc5 block DNA replication between the two meiotic divisions by phosphorylation of several components involved in helicase-loading and an essential helicase-activation protein Sld2 (Phizicky *et al.*, 2018). Notably, Cdk and Cdc7 kinases function in a concerted manner in phosphorylation of Mcm2 in human cells (Cho *et al.*, 2006). Phosphorylation of S26 and S40 of Mcm2 by both Cdk and Cdc7 kinases have been implicated in DNA replication (Cho *et al.*, 2006).

Our study revealed that the *in vivo* interaction of Cdc5 and Cse4 is cell cycle regulated

and occurs in mitotic cells. The mitotic interaction of Cdc5 with Cse4 is coincident with the cell cycle regulated association of Cdc5 with *CEN* chromatin in metaphase and early anaphase cells, but lack of enrichment in telophase and G1 cells (Mishra *et al.*, 2016). Notably, the mitotic interaction of Cdc5 with Cse4 also correlates with the increased levels of phosphorylated Cse4 observed at *CEN* in cells arrested in G2/M stage of the cell cycle but not in G1 (Boeckmann *et al.*, 2013). Taken together, our results show that the phosphorylation pattern of Cse4 overlaps with the *CEN* association and activity of Cdc5 kinase during mitosis (Charles *et al.*, 1998; Alexandru *et al.*, 2001; Hornig and Uhlmann, 2004; Mishra *et al.*, 2016). The cell cycle dependent phosphorylation of Cse4 is physiologically important as constitutive phosphorylation of Cse4 is detrimental for cell growth as *cse4-9SD* phosphomimetic mutant cannot rescue the growth of a *cse4*Δ strain. Consistent with this hypothesis, we have shown that constitutive association of Cdc5 with Cse4 results in growth defects. We propose that cell cycle regulated association of Cdc5 facilitates dynamic phosphorylation of Cse4 for the maintenance of proper kinetochore structure and faithful chromosome segregation. Previous studies have showed that dynamic phosphorylation of kinetochore proteins, such as Cse4, Dam1, Ndc80, Dsn1 and Ask1 destabilizes defective kinetochore to promote biorientation by interaction with microtubules (Cheeseman *et al.*, 2002; Westermann *et al.*, 2003; Akiyoshi and Biggins, 2010; Boeckmann *et al.*, 2013; Jin *et al.*, 2017).

Defect in Cse4 phosphorylation (*cse4-9SA*) causes increased errors in chromosome segregation when combined with *mcm21Δ* indicating a role for Cse4 phosphorylation in the maintenance of kinetochore integrity during mitosis. This is not surprising given that

cse4-4SA and *cse4-S33A* exhibit phenotypic defects only when combined with *dam1* and *hhf1* mutants, respectively (Boeckmann *et al.*, 2013; Hoffmann *et al.*, 2018). Moreover, both Cse4 and Mcm21 have roles in *CEN* structure-function, spindle biorientation, and maintenance of *CEN* cohesion (Meluh *et al.*, 1998; Ng *et al.*, 2009; Pekgoz Altunkaya *et al.*, 2016; Tsabar *et al.*, 2016; Mishra *et al.*, 2018). Our results showing significantly reduced levels of Mif2 at *CEN* in *cse4-9SA mcm21Δ* compared to the single mutant (*cse4-9SA* or *mcm21Δ*) further supports a role for phosphorylation of Cse4 in the assembly of *CEN* chromatin and kinetochore function. As *CEN* localization of Mif2 requires Cse4 (Ho *et al.*, 2014), the reduced levels of Mif2 at *CEN* in *cse4-9SA mcm21Δ* strain may be a reflection of altered association of *cse4-9SA* at the *CEN*. A previous study has shown that Mif2 and Cse4 are required for the association of cohesins at the centromeres (Eckert *et al.*, 2007). Moreover, deletion of *MCM21* affects the assembly of Ctf19 complex at the kinetochores (Lang *et al.*, 2018). In agreement with these reports, our results showed reduced levels of Mcd1/Scc1 at the *CEN* in *cse4-9SA mcm21*Δ strains that exhibited reduction in Mif2 at the *CENs*. We propose that Cdc5-mediated phosphorylation of Cse4 contributes to faithful chromosome segregation.

In summary, we have shown that Cdc5 interacts with Cse4 *in vivo* in a cell cycle dependent manner, and this interaction is essential for cell viability. We provide the first evidence for a functional role for Cdc5-mediated phosphorylation of Cse4 in faithful chromosome segregation. It is notable that Plk1 (Cdc5 homolog in humans) phosphorylates kinetochore protein Mis18BP1, which in turn promotes the *CEN* assembly of newly synthesized CENP-A (McKinley and Cheeseman, 2014). However, it

remains unexplored whether CENP-A is a direct substrate for Plk1 in human cells. Identification and characterization of additional Plk1 substrates at the human kinetochores will allow us to better understand the role of epigenetic modifications, such as phosphorylation in the assembly of a functional kinetochore for chromosomal stability.

MATERIALS AND METHODS

Yeast strains, plasmids, and growth conditions

Yeast strains were grown in yeast peptone dextrose medium (1% yeast extract, 2% Bacto-peptone, 2% glucose; YPD) or in synthetic medium with supplements to allow for the selection of plasmids being used. Yeast strains, and plasmids are listed in Table 1.

Chromosome segregation assay

The fidelity of chromosome segregation was measured using a colony color assay as described previously (Spencer *et al.*, 1990). In this assay, loss of non-essential reporter a chromosome fragment (CF) leads to red sectors in an otherwise a white colony. Wild type, *cse4-S33A, cse4-9SA, mcm21Δ, cse4-9SA mcm21Δ, cse4-S33A mcm21Δ, ctf19Δ,* and *cse4-9SA ctf19Δ* strains carrying CF were grown in medium selective for the CF to the logarithmic phase, and plated on complete synthetic medium with limiting adenine at 33ºC to allow the loss of CF. About 1000 colonies of three transformants were examined for each strain. The frequency of CF loss was determined by counting the number of colonies that were at least half red representing the loss of the CF during the first mitotic cell division cycle.

Chromatin immunoprecipitation (ChIP) and quantitative PCR (qPCR)

ChIP experiments were performed with three biological replicates following the procedure as described previously (Mishra *et al.*, 2007; Mishra *et al.*, 2011). Antibodies used to capture protein-DNA complexes were α-GFP sepharose (ab69314, AbCam), α-Mif2 (a gift from Pam Meluh), α-Cdc5 (custom made by the D'Amours laboratory; (Ratsima *et al.*, 2011; Robellet *et al.*, 2015)), and α-HA agarose (A2095, Sigma Aldrich). ChIP-qPCR was performed in 7500 Fast Real Time PCR System using Fast SYBR Green Master Mix (Applied Biosystems, Foster City, CA) with the following conditions: 95ºC for 20 sec, followed by 40 cycles of 95ºC for 3 sec, 60ºC for 30 sec. The enrichment was determined as percent input using the $_{\Delta\Delta}C_T$ method (Livak and Schmittgen, 2001). Primer sequences are listed in Table 2.

Cell cycle synchronization, immunoprecipitation (IP) and Western blotting

Strains were grown to logarithmic phase at 30°C in synthetic complete (SC) medium lacking tryptophan (SC-Trp) and further incubated for 2 hours to synchronize cells in G1 (3 μM alpha factor treatment), S (0.2 M hydroxyurea treatment), and G2/M (20 μg/ml nocodazole treatment) stages of the cell cycle. Cells were collected, washed with water, grown for 1 hour in SC-Trp with galactose + raffinose (2% each) medium to induce the expression of Flag-tagged Cse4 expressed from the *GAL1* promoter. Culture media also contained chemicals described above to keep the cells in G1, S and G2/M stages of the cell cycle. Samples were collected for nuclear morphology, DNA content, and IP analyses. IP experiments were performed using α-Flag agarose antibodies (A2022, Sigma

Aldrich) as described previously (Mishra *et al.*, 2011; Mishra *et al.*, 2018). Whole cell extracts were prepared with the TCA method (Kastenmayer *et al.*, 2005), and quantified using Bio-Rad DC protein quantitation assay (Bio-Rad Laboratories, Hercules, CA). Protein samples were resolved on SDS polyacrylamide gels, and transferred to nitrocellulose membrane. Primary antibodies used for Western blotting were α-HA (H6908, Sigma Aldrich), α-Flag (F3165, Sigma Aldrich), α-GFP (11814460001, Roche), α-Mif2 (a gift from Pam Meluh), and α-Tub2 (custom made by the Basrai laboratory). Secondary antibodies: HRP-conjugated sheep α-rabbit IgG (NA934V) and HRP-conjugated sheep α-mouse IgG (NA931V) were obtained from Amersham Biosciences (United Kingdom).

In vitro kinase assay and mass spectrometry

In vitro kinase assay and mass spectrometry were carried out using Cse4 produced and purified from *Escherichia coli* as described previously (Luger *et al.*, 1997; Boeckmann *et al.*, 2013). Wild type Cdc5 and its kinase dead derivative (K100M) were purified from yeast as previously described (Ratsima *et al.*, 2011). *In vitro* kinase assays were performed using radiolabeled ATP in 20-µl reaction volume containing 0.5 µg Cse4, 40 ng Cdc5, 2 mM dithiothreitol, 1 mM $MgCl_2$, 25 mM Tris-HCl pH 7.5, 100 µM ATP, and 1 µCi of [γ-^{32}P]ATP. Control reactions were performed using purified histone H3 with Cdc5. Reactions were incubated at 30°C for 60 min, stopped with 5 µl of 4 × NuPAGE LDS loading buffer (Life Technologies, Grand Island, NY), boiled for 5 min at 95°C, and were run on 4–12% Bis-Tris SDS-polyacrylamide gels (Invitrogen). Gels were stained with Coomassie blue, and radiolabeled proteins were visualized using a Storm Detector

Model 860 (Molecular Dynamics, USA). For mass spectrometry, *in vitro* kinase assay with and without Cdc5 were performed as described previously (Boeckmann *et al.*, 2013). Reactions were analyzed on 4–12% Bis-Tris SDS-polyacrylamide gels (Invitrogen), Cse4 bands were excised, and subjected to mass spectrometry following procedures described previously (Waybright *et al.*, 2008; Boeckmann *et al.*, 2013). The *Saccharomyces cerevisiae* proteome database (www.expasy.org) was used for data analysis.

***In vivo* assay for phosphorylation of Cse4**

The levels of Cse4 phosphorylation *in vivo* were determined using procedures and αp-Cse4 antibodies as described previously (Boeckmann *et al.*, 2013). Wild type and *cdc5-99* strains carrying *6HIS-3HA-CSE4* expressed from *GAL1* promoter were grown in 1x SC-URA with 2% glucose media at 25°C. Cells were washed with water and inoculated into 1x SC-URA with galactose + raffinose (2% each) to induce the expression of *6HIS-3HA-CSE4* and 1.5 µM α-factor to synchronize cells in G1. Cells were collected, washed with water, and released into pheromone free media (1x SC-URA with 2% galactose + raffinose) at 25° and 37°C. Cell cycle progression was monitored by microscopic examination of nuclear and cell morphology. Samples for FACS and affinity pull down were collected ~110 min after G1 release when majority of cells were at metaphase (~70%) stage of the cell cycle. Cells were dissolved in lysis buffer (6 M guanidine chloride, 0.5 M NaCl, 0.1 M Tris, pH 8.0), and whole cell extracts were prepared using

FastPrep 24-5G bead beater (40 sec, 10 times, 1 min interval between bursts; MP Biomedicals) at 4°C. Whole cell extracts were clarified by centrifugation, and incubated with nickel-charged superflow NTA agarose (Qiagen, Valencia, CA) for 16 hours at 4°C. Beads were centrifuged, and washed once with lysis buffer, followed by three washes with washing buffer (100 mM Tris-Cl, pH 8.0, 20% glycerol, 1 mM phenylmethylsulfonyl fluoride; 5 min each wash at the room temperature). The bound protein was eluted by boiling at 100°C for 10 min in 2× Laemmli buffer with 200 mM imidazole. Protein samples were resolved by SDS–PAGE on 4–12% Bis-Tris SDS-polyacrylamide gels, and transferred to nitrocellulose membranes. Blots were washed with 1x TBST (Tris-buffered saline plus 0.1% Tween 20) three times for 5 min, blocked for 15 min in 1x TBST containing 5% skimmed milk. Western blot analysis was done using primary antibodies: α-HA (1/1000 dilutions; 12CA5, Roche) or αp-Cse4 (1/250 dilutions, (Boeckmann *et al.*, 2013)) in 1x TBST with 5% milk. Secondary antibodies used were: HRP-conjugated sheep α-rabbit IgG (NA934V) and HRP-conjugated sheep α-mouse IgG (NA931V). Signal intensities from Western blots were quantified using ImageJ (Schneider *et al.*, 2012).

Extraction of nuclei and *DraI* accessibility assays

Extraction of nuclei and *DraI* accessibility experiments were as described previously (Mishra *et al.*, 2013) with some modifications. Briefly, cells were dissolved in spheroplasting buffer (20 mM Hepes pH 7.4, 1.2 M sorbitol, 0.5 mM PMSF), added *β*-mercaptoethanol (5 µl/ml cell suspension; Sigma Aldrich) and Zymolyase 100T (0.04 mg/ml cell suspension; MP Biomedicals); and incubated at 37°C for spheroplast

preparation. Spheroplasting was monitored by measuring OD_{800} in 1% SDS and reactions were stopped by washing in post-spheroplasting buffer (20 mM Pipes pH 6.8, 1.2 M sorbitol, 1 mM $MgCl_2$, 1 mM PMSF) when >90% spheroplasting was achieved. Spheroplasts were lysed in 20 mM Pipes (pH 6.8), 18% Ficoll 400, 0.5 mM $MgCl_2$, 1 mM PMSF. Nuclei were released by vortexing for 10 min at 4°C, and harvested by centrifugation through a glycerol/Ficoll gradient cushion (20% Glycerol, 20 mM Pipes pH 6.8, 7% Ficoll 400, 0.5 mM $MgCl_2$, 1 mM PMSF). Nuclei were washed and resuspended in *DraI* buffer (1.0 M sorbitol, 20 mM Pipes pH 6.8, 0.1 mM $CaCl_2$, 1 mM PMSF, 0.5 mM $MgCl_2$). The nuclei concentrations were determined by measuring OD_{260} in alkaline SDS buffer (0.2 N NaOH, 1% SDS). Equal volume of nuclei (100 µl) from each sample were pre-warmed for 5 min at 37°C followed by the addition of 100 units of *DraI* (New England BioLabs) for 30 min. Restriction digestion was stopped by adjusting aliquots to 2% SDS, 20 mM EDTA. DNA was isolated after extraction first with phenol, chloroform, isoamyl alcohol (twice), treated with RNase A and Proteinase K, followed by extraction with chloroform. DNA was precipitated in ethanol at -20°C, collected by centrifugation, dissolved in 1x TE (pH 8.0), and was used in qPCR to determine the susceptibility of *CEN3* chromatin to digestion by *DraI* using Fast SYBR-Green Master Mix (Applied Biosystems, CA), and PCR primers flanking *CEN3* and a control region *ADP1* (Mishra *et al.*, 2013). The amplification conditions for *CEN3* were: initial denaturation at 95°C for 20 sec followed by cycling of 95°C for 3 sec, 60°C for 30 sec (data acquisition step); and ADP1 were: initial denaturation at 95°C for 30 sec followed by cycling of 95°C for 15 sec, 54°C for 15 sec, 68°C for 60 sec (data acquisition step) in a 7500 Fast-Real Time PCR System (Applied Biosystems, CA). The fraction of DNA

cleaved by *DraI* was determined by normalization of C_T values to those obtained from the no *DraI* control.

Synthetic physical interaction (SPI) and microscopy

SPI screens were performed as previously described (Olafsson and Thorpe, 2015, 2018). Briefly, a Universal Donor Strain, which contains conditional *GAL-CEN* centromeres, was transformed separately with the control and experimental plasmids (expressing either Cdc5-GBP, cdc5kd-GBP (a kinase-dead version) or GBP alone; all under the control of a constitutive *CUP1* promoter). These universal donor strains were then mated with members of the GFP collection arrayed with 16 replicates on 1536-colony rectangular agar plates using a pinning robot (ROTOR robot, Singer Instruments, UK). The resulting diploids were put through a series of sequential selection steps to maintain the plasmid, while destabilizing and then removing the chromosomes of the universal donor strain. The resulting plates were scanned using a desktop flatbed scanner (Epson V750 Pro, Seiko Epson Corporation, Japan). Colony sizes were assessed and the resulting data analyzed using the ScreenMill suite of software (Dittmar *et al.*, 2010). Flourescence imaging was performed on yeast cells embedded in 0.7% low melting point agarose dissolved in growth medium. The cells were imaged with a Zeiss Axioimager Z2 microscope using a 63x 1.4NA oil immersion lens, illuminated with a Zeiss Colibri LED light source (GFP=470 nm, RFP = 590 nm). Bright field contrast was enhanced using differential interference prisms. Images were captured using a Flash 4.0 LT CMOS camera with 6.5 µm pixels binned 2x2 (Hamamatsu photonics, Japan).

ACKNOWLEDGEMENTS

We are highly thankful to Drs. Sue Biggins, Orna Cohen-Fix, and Vincent Guacci for strains, plasmids and helpful suggestions; Kathy McKinnon of the National Cancer Institute Vaccine Branch FACS Core for assistance with FACS; Mirela Pascariu for the purification of Cdc5 kinase; Timothy Waybright and Timothy Veenstra of the Frederick National Laboratory for Cancer Research for assistance with mass spectrometry; and the members of the Basrai laboratory for technical assistance and helpful discussions. PKM, LB, TJW, ZMJ, LED, and MAB were supported by the Intramural Research Program of the National Cancer Institute, National Institutes of Health; DD is supported by the Canadian Institutes of Health Research (CIHR; MOP 82912, MOP 136788, PJT 148969), and by a Canada Research Chair in Chromatin Dynamics & Genome Architecture (Tier 1); and GO and PHT were supported by the Queen Mary University of London, and the Francis Crick Institute, which receives its core funding from Cancer Research UK (FC001003), the UK Medical Research Council (FC001003), and the Wellcome Trust (FC001003).

REFERENCES

Akiyoshi, B., and Biggins, S. (2010). Cdc14-dependent dephosphorylation of a kinetochore protein prior to anaphase in Saccharomyces cerevisiae. Genetics *186*, 1487-1491.

Alexandru, G., Uhlmann, F., Mechtler, K., Poupart, M.A., and Nasmyth, K. (2001). Phosphorylation of the cohesin subunit Scc1 by Polo/Cdc5 kinase regulates sister chromatid separation in yeast. Cell *105*, 459-472.

Asano, S., Park, J.E., Sakchaisri, K., Yu, L.R., Song, S., Supavilai, P., Veenstra, T.D., and Lee, K.S. (2005). Concerted mechanism of Swe1/Wee1 regulation by multiple kinases in budding yeast. EMBO J *24*, 2194-2204.

Au, W.C., Dawson, A.R., Rawson, D.W., Taylor, S.B., Baker, R.E., and Basrai, M.A. (2013). A Novel Role of the N-Terminus of Budding Yeast Histone H3 Variant Cse4 in Ubiquitin-Mediated Proteolysis. Genetics *194*, 513-518.

Biggins, S. (2013). The composition, functions, and regulation of the budding yeast kinetochore. Genetics *194*, 817-846.

Boeckmann, L., Takahashi, Y., Au, W.C., Mishra, P.K., Choy, J.S., Dawson, A.R., Szeto, M.Y., Waybright, T.J., Heger, C., McAndrew, C., Goldsmith, P.K., Veenstra, T.D., Baker, R.E., and Basrai, M.A. (2013). Phosphorylation of centromeric histone H3 variant regulates chromosome segregation in Saccharomyces cerevisiae. Mol Biol Cell *24*, 2034-2044.

Botchkarev, V.V., Jr., and Haber, J.E. (2018). Functions and regulation of the Polo-like kinase Cdc5 in the absence and presence of DNA damage. Curr Genet *64*, 87-96.

Brooker, A.S., and Berkowitz, K.M. (2014). The roles of cohesins in mitosis, meiosis, and human health and disease. Methods Mol Biol *1170*, 229-266.

Brown, M.T., Goetsch, L., and Hartwell, L.H. (1993). MIF2 is required for mitotic spindle integrity during anaphase spindle elongation in Saccharomyces cerevisiae. J Cell Biol *123*, 387-403.

Burrack, L.S., and Berman, J. (2012). Flexibility of centromere and kinetochore structures. Trends Genet *28*, 204-212.

Buvelot, S., Tatsutani, S.Y., Vermaak, D., and Biggins, S. (2003). The budding yeast Ipl1/Aurora protein kinase regulates mitotic spindle disassembly. J Cell Biol *160*, 329-339.

Charles, J.F., Jaspersen, S.L., Tinker-Kulberg, R.L., Hwang, L., Szidon, A., and Morgan, D.O. (1998). The Polo-related kinase Cdc5 activates and is destroyed by the mitotic cyclin destruction machinery in S. cerevisiae. Curr Biol *8*, 497-507.

Cheeseman, I.M., Anderson, S., Jwa, M., Green, E.M., Kang, J., Yates, J.R., 3rd, Chan, C.S., Drubin, D.G., and Barnes, G. (2002). Phospho-regulation of kinetochore-microtubule attachments by the Aurora kinase Ipl1p. Cell *111*, 163-172.

Chen, Y., Baker, R.E., Keith, K.C., Harris, K., Stoler, S., and Fitzgerald-Hayes, M. (2000). The N terminus of the centromere H3-like protein Cse4p performs an essential function distinct from that of the histone fold domain. Mol Cell Biol *20*, 7037-7048.

Cho, U.S., Corbett, K.D., Al-Bassam, J., Bellizzi, J.J., 3rd, De Wulf, P., Espelin, C.W., Miranda, J.J., Simons, K., Wei, R.R., Sorger, P.K., and Harrison, S.C. (2010). Molecular structures and interactions in the yeast kinetochore. Cold Spring Harb Symp Quant Biol *75*, 395-401.

Cho, W.H., Lee, Y.J., Kong, S.I., Hurwitz, J., and Lee, J.K. (2006). CDC7 kinase phosphorylates serine residues adjacent to acidic amino acids in the minichromosome maintenance 2 protein. Proc Natl Acad Sci U S A *103*, 11521-11526.

Choy, J.S., Acuna, R., Au, W.C., and Basrai, M.A. (2011). A role for histone H4K16 hypoacetylation in Saccharomyces cerevisiae kinetochore function. Genetics *189*, 11-21.

Clarke, L., and Carbon, J. (1980). Isolation of a yeast centromere and construction of functional small circular chromosomes. Nature *287*, 504-509.

Cohen, R.L., Espelin, C.W., De Wulf, P., Sorger, P.K., Harrison, S.C., and Simons, K.T. (2008). Structural and functional dissection of Mif2p, a conserved DNA-binding kinetochore protein. Mol Biol Cell *19*, 4480-4491.

Dittmar, J.C., Reid, R.J., and Rothstein, R. (2010). ScreenMill: a freely available software suite for growth measurement, analysis and visualization of high-throughput screen data. BMC Bioinformatics *11*, 353.

Eckert, C.A., Gravdahl, D.J., and Megee, P.C. (2007). The enhancement of pericentromeric cohesin association by conserved kinetochore components promotes high-fidelity chromosome segregation and is sensitive to microtubule-based tension. Genes Dev *21*, 278-291.

Haase, J., Mishra, P.K., Stephens, A., Haggerty, R., Quammen, C., Taylor, R.M., 2nd, Yeh, E., Basrai, M.A., and Bloom, K. (2013). A 3D map of the yeast kinetochore reveals the presence of core and accessory centromere-specific histone. Curr Biol *23*, 1939-1944.

Henikoff, S., Ahmad, K., Platero, J.S., and van Steensel, B. (2000). Heterochromatic deposition of centromeric histone H3-like proteins. Proc Natl Acad Sci U S A *97*, 716-721.

Hewawasam, G., Shivaraju, M., Mattingly, M., Venkatesh, S., Martin-Brown, S., Florens, L., Workman, J.L., and Gerton, J.L. (2010). Psh1 is an E3 ubiquitin ligase that targets the centromeric histone variant Cse4. Mol Cell *40*, 444-454.

Hinshaw, S.M., Makrantoni, V., Harrison, S.C., and Marston, A.L. (2017). The Kinetochore Receptor for the Cohesin Loading Complex. Cell *171*, 72-84 e13.

Ho, K.H., Tsuchiya, D., Oliger, A.C., and Lacefield, S. (2014). Localization and Function of Budding Yeast CENP-A Depends upon Kinetochore Protein Interactions and Is Independent of Canonical Centromere Sequence. Cell reports *9*, 2027-2033.

Hoffmann, G., Samel-Pommerencke, A., Weber, J., Cuomo, A., Bonaldi, T., and Ehrenhofer-Murray, A.E. (2018). A role for CENP-A/Cse4 phosphorylation on serine 33 in deposition at the centromere. FEMS Yeast Res *18*.

Hornig, N.C., and Uhlmann, F. (2004). Preferential cleavage of chromatin-bound cohesin after targeted phosphorylation by Polo-like kinase. EMBO J *23*, 3144-3153.

Huh, W.K., Falvo, J.V., Gerke, L.C., Carroll, A.S., Howson, R.W., Weissman, J.S., and O'Shea, E.K. (2003). Global analysis of protein localization in budding yeast. Nature *425*, 686-691.

Jin, F., Bokros, M., and Wang, Y. (2017). The phosphorylation of a kinetochore protein Dam1 by Aurora B/Ipl1 kinase promotes chromosome bipolar attachment in yeast. Sci Rep *7*, 11880.

Kastenmayer, J.P., Lee, M.S., Hong, A.L., Spencer, F.A., and Basrai, M.A. (2005). The C-terminal half of Saccharomyces cerevisiae Mad1p mediates spindle checkpoint function, chromosome transmission fidelity and CEN association. Genetics *170*, 509-517.

Keith, K.C., Baker, R.E., Chen, Y., Harris, K., Stoler, S., and Fitzgerald-Hayes, M. (1999). Analysis of primary structural determinants that distinguish the centromere-specific function of histone variant Cse4p from histone H3. Mol Cell Biol *19*, 6130-6139.

Laloraya, S., Guacci, V., and Koshland, D. (2000). Chromosomal addresses of the cohesin component Mcd1p. J Cell Biol *151*, 1047-1056.

Lang, J., Barber, A., and Biggins, S. (2018). An assay for de novo kinetochore assembly reveals a key role for the CENP-T pathway in budding yeast. eLife *7*.

Lechner, J., and Carbon, J. (1991). A 240 kd multisubunit protein complex, CBF3, is a major component of the budding yeast centromere. Cell *64*, 717-725.

Livak, K.J., and Schmittgen, T.D. (2001). Analysis of relative gene expression data using real-time quantitative PCR and the 2(-Delta Delta C(T)) Method. Methods *25*, 402-408.

Luger, K., Rechsteiner, T.J., Flaus, A.J., Waye, M.M., and Richmond, T.J. (1997). Characterization of nucleosome core particles containing histone proteins made in bacteria. J Mol Biol *272*, 301-311.

McKinley, K.L., and Cheeseman, I.M. (2014). Polo-like kinase 1 licenses CENP-A deposition at centromeres. Cell *158*, 397-411.

Meluh, P.B., and Koshland, D. (1995). Evidence that the MIF2 gene of Saccharomyces cerevisiae encodes a centromere protein with homology to the mammalian centromere protein CENP-C. Mol Biol Cell *6*, 793-807.

Meluh, P.B., Yang, P., Glowczewski, L., Koshland, D., and Smith, M.M. (1998). Cse4p is a component of the core centromere of Saccharomyces cerevisiae. Cell *94*, 607-613.

Mishra, P.K., Au, W.C., Choy, J.S., Kuich, P.H., Baker, R.E., Foltz, D.R., and Basrai, M.A. (2011). Misregulation of Scm3p/HJURP causes chromosome instability in Saccharomyces cerevisiae and human cells. PLoS Genet *7*, e1002303.

Mishra, P.K., Baum, M., and Carbon, J. (2007). Centromere size and position in Candida albicans are evolutionarily conserved independent of DNA sequence heterogeneity. Molecular genetics and genomics : MGG *278*, 455-465.

Mishra, P.K., Ciftci-Yilmaz, S., Reynolds, D., Au, W.C., Boeckmann, L., Dittman, L.E., Jowhar, Z., Pachpor, T., Yeh, E., Baker, R.E., Hoyt, M.A., D'Amours, D., Bloom, K., and Basrai, M.A. (2016). Polo kinase Cdc5 associates with centromeres to facilitate the removal of centromeric cohesin during mitosis. Mol Biol Cell *27*, 2286-2300.

Mishra, P.K., Ottmann, A.R., and Basrai, M.A. (2013). Structural integrity of centromeric chromatin and faithful chromosome segregation requires Pat1. Genetics *195*, 369-379.

Mishra, P.K., Thapa, K.S., Chen, P., Wang, S., Hazbun, T.R., and Basrai, M.A. (2018). Budding yeast CENP-A(Cse4) interacts with the N-terminus of Sgo1 and regulates its association with centromeric chromatin. Cell Cycle *17*, 11-23.

Musacchio, A., and Desai, A. (2017). A Molecular View of Kinetochore Assembly and Function. Biology (Basel) *6*.

Ng, T.M., Waples, W.G., Lavoie, B.D., and Biggins, S. (2009). Pericentromeric sister chromatid cohesion promotes kinetochore biorientation. Mol Biol Cell *20*, 3818-3827.

Ohkuni, K., Takahashi, Y., Fulp, A., Lawrimore, J., Au, W.C., Pasupala, N., Levy-Myers, R., Warren, J., Strunnikov, A., Baker, R.E., Kerscher, O., Bloom, K., and Basrai, M.A. (2016). SUMO-Targeted Ubiquitin Ligase (STUbL) Slx5 regulates proteolysis of

centromeric histone H3 variant Cse4 and prevents its mislocalization to euchromatin. Mol Biol Cell.

Olafsson, G., and Thorpe, P.H. (2015). Synthetic physical interactions map kinetochore regulators and regions sensitive to constitutive Cdc14 localization. Proc Natl Acad Sci U S A *112*, 10413-10418.

Olafsson, G., and Thorpe, P.H. (2016). Synthetic Physical Interactions Map Kinetochore-Checkpoint Activation Regions. G3 (Bethesda) *6*, 2531-2542.

Olafsson, G., and Thorpe, P.H. (2018). Rewiring the Budding Yeast Proteome using Synthetic Physical Interactions. Methods Mol Biol *1672*, 599-612.

Ortiz, J., Stemmann, O., Rank, S., and Lechner, J. (1999). A putative protein complex consisting of Ctf19, Mcm21, and Okp1 represents a missing link in the budding yeast kinetochore. Genes Dev *13*, 1140-1155.

Park, C.J., Park, J.E., Karpova, T.S., Soung, N.K., Yu, L.R., Song, S., Lee, K.H., Xia, X., Kang, E., Dabanoglu, I., Oh, D.Y., Zhang, J.Y., Kang, Y.H., Wincovitch, S., Huffaker, T.C., Veenstra, T.D., McNally, J.G., and Lee, K.S. (2008). Requirement for the budding yeast polo kinase Cdc5 in proper microtubule growth and dynamics. Eukaryotic cell *7*, 444-453.

Pearson, C.G., Yeh, E., Gardner, M., Odde, D., Salmon, E.D., and Bloom, K. (2004). Stable kinetochore-microtubule attachment constrains centromere positioning in metaphase. Curr Biol *14*, 1962-1967.

Pekgoz Altunkaya, G., Malvezzi, F., Demianova, Z., Zimniak, T., Litos, G., Weissmann, F., Mechtler, K., Herzog, F., and Westermann, S. (2016). CCAN Assembly Configures

Composite Binding Interfaces to Promote Cross-Linking of Ndc80 Complexes at the Kinetochore. Curr Biol *26*, 2370-2378.

Phizicky, D.V., Berchowitz, L.E., and Bell, S.P. (2018). Multiple kinases inhibit origin licensing and helicase activation to ensure reductive cell division during meiosis. eLife *7*.

Rahal, R., and Amon, A. (2008). The Polo-like kinase Cdc5 interacts with FEAR network components and Cdc14. Cell Cycle *7*, 3262-3272.

Ranjitkar, P., Press, M.O., Yi, X., Baker, R., MacCoss, M.J., and Biggins, S. (2010). An E3 ubiquitin ligase prevents ectopic localization of the centromeric histone H3 variant via the centromere targeting domain. Mol Cell *40*, 455-464.

Ratsima, H., Ladouceur, A.M., Pascariu, M., Sauve, V., Salloum, Z., Maddox, P.S., and D'Amours, D. (2011). Independent modulation of the kinase and polo-box activities of Cdc5 protein unravels unique roles in the maintenance of genome stability. Proc Natl Acad Sci U S A *108*, E914-923.

Reid, R.J., Gonzalez-Barrera, S., Sunjevaric, I., Alvaro, D., Ciccone, S., Wagner, M., and Rothstein, R. (2011). Selective ploidy ablation, a high-throughput plasmid transfer protocol, identifies new genes affecting topoisomerase I-induced DNA damage. Genome research *21*, 477-486.

Robellet, X., Thattikota, Y., Wang, F., Wee, T.L., Pascariu, M., Shankar, S., Bonneil, E., Brown, C.M., and D'Amours, D. (2015). A high-sensitivity phospho-switch triggered by Cdk1 governs chromosome morphogenesis during cell division. Genes Dev *29*, 426-439.

Roccuzzo, M., Visintin, C., Tili, F., and Visintin, R. (2015). FEAR-mediated activation of Cdc14 is the limiting step for spindle elongation and anaphase progression. Nat Cell Biol *17*, 251-261.

Rossio, V., Galati, E., Ferrari, M., Pellicioli, A., Sutani, T., Shirahige, K., Lucchini, G., and Piatti, S. (2010). The RSC chromatin-remodeling complex influences mitotic exit and adaptation to the spindle assembly checkpoint by controlling the Cdc14 phosphatase. J Cell Biol *191*, 981-997.

Rothbauer, U., Zolghadr, K., Muyldermans, S., Schepers, A., Cardoso, M.C., and Leonhardt, H. (2008). A versatile nanotrap for biochemical and functional studies with fluorescent fusion proteins. Mol Cell Proteomics *7*, 282-289.

Samel, A., Cuomo, A., Bonaldi, T., and Ehrenhofer-Murray, A.E. (2012). Methylation of CenH3 arginine 37 regulates kinetochore integrity and chromosome segregation. Proc Natl Acad Sci U S A *109*, 9029-9034.

Santaguida, S., and Amon, A. (2015). Short- and long-term effects of chromosome mis-segregation and aneuploidy. Nat Rev Mol Cell Biol *16*, 473-485.

Saunders, M.J., Yeh, E., Grunstein, M., and Bloom, K. (1990). Nucleosome depletion alters the chromatin structure of Saccharomyces cerevisiae centromeres. Mol Cell Biol *10*, 5721-5727.

Schneider, C.A., Rasband, W.S., and Eliceiri, K.W. (2012). NIH Image to ImageJ: 25 years of image analysis. Nat Methods *9*, 671-675.

Snead, J.L., Sullivan, M., Lowery, D.M., Cohen, M.S., Zhang, C., Randle, D.H., Taunton, J., Yaffe, M.B., Morgan, D.O., and Shokat, K.M. (2007). A coupled chemical-genetic and bioinformatic approach to Polo-like kinase pathway exploration. Chemistry & biology *14*, 1261-1272.

Spencer, F., Gerring, S.L., Connelly, C., and Hieter, P. (1990). Mitotic chromosome transmission fidelity mutants in Saccharomyces cerevisiae. Genetics *124*, 237-249.

St-Pierre, J., Douziech, M., Bazile, F., Pascariu, M., Bonneil, E., Sauve, V., Ratsima, H., and D'Amours, D. (2009). Polo kinase regulates mitotic chromosome condensation by hyperactivation of condensin DNA supercoiling activity. Mol Cell *34*, 416-426.

Stoler, S., Keith, K.C., Curnick, K.E., and Fitzgerald-Hayes, M. (1995). A mutation in CSE4, an essential gene encoding a novel chromatin-associated protein in yeast, causes chromosome nondisjunction and cell cycle arrest at mitosis. Genes Dev *9*, 573-586.

Strunnikov, A.V., Kingsbury, J., and Koshland, D. (1995). CEP3 encodes a centromere protein of Saccharomyces cerevisiae. J Cell Biol *128*, 749-760.

Sullivan, K.F., Hechenberger, M., and Masri, K. (1994). Human CENP-A contains a histone H3 related histone fold domain that is required for targeting to the centromere. J Cell Biol *127*, 581-592.

Takahashi, K., Chen, E.S., and Yanagida, M. (2000). Requirement of Mis6 centromere connector for localizing a CENP-A-like protein in fission yeast. Science *288*, 2215-2219.

Tsabar, M., Haase, J., Harrison, B., Snider, C.E., Eldridge, B., Kaminsky, L., Hine, R.M., Haber, J.E., and Bloom, K. (2016). A Cohesin-Based Partitioning Mechanism Revealed upon Transcriptional Inactivation of Centromere. PLoS Genet *12*, e1006021.

Tukenmez, H., Magnussen, H.M., Kovermann, M., Bystrom, A., and Wolf-Watz, M. (2016). Linkage between Fitness of Yeast Cells and Adenylate Kinase Catalysis. PLoS One *11*, e0163115.

Uhlmann, F., Wernic, D., Poupart, M.A., Koonin, E.V., and Nasmyth, K. (2000). Cleavage of cohesin by the CD clan protease separin triggers anaphase in yeast. Cell *103*, 375-386.

Van Hooser, A.A., Ouspenski, II, Gregson, H.C., Starr, D.A., Yen, T.J., Goldberg, M.L., Yokomori, K., Earnshaw, W.C., Sullivan, K.F., and Brinkley, B.R. (2001). Specification of kinetochore-forming chromatin by the histone H3 variant CENP-A. J Cell Sci *114*, 3529-3542.

Verdaasdonk, J.S., and Bloom, K. (2011). Centromeres: unique chromatin structures that drive chromosome segregation. Nat Rev Mol Cell Biol *12*, 320-332.

Verdaasdonk, J.S., Gardner, R., Stephens, A.D., Yeh, E., and Bloom, K. (2012). Tension-dependent nucleosome remodeling at the pericentromere in yeast. Mol Biol Cell *23*, 2560-2570.

Walters, A.D., May, C.K., Dauster, E.S., Cinquin, B.P., Smith, E.A., Robellet, X., D'Amours, D., Larabell, C.A., and Cohen-Fix, O. (2014). The yeast polo kinase Cdc5 regulates the shape of the mitotic nucleus. Curr Biol *24*, 2861-2867.

Waybright, T., Gillette, W., Esposito, D., Stephens, R., Lucas, D., Hartley, J., and Veenstra, T. (2008). Identification of highly expressed, soluble proteins using an improved, high-throughput pooled ORF expression technology. Biotechniques *45*, 307-315.

Weber, S.A., Gerton, J.L., Polancic, J.E., DeRisi, J.L., Koshland, D., and Megee, P.C. (2004). The kinetochore is an enhancer of pericentric cohesin binding. PLoS Biol *2*, E260.

Westermann, S., Cheeseman, I.M., Anderson, S., Yates, J.R., 3rd, Drubin, D.G., and Barnes, G. (2003). Architecture of the budding yeast kinetochore reveals a conserved molecular core. J Cell Biol *163*, 215-222.

Widlund, P.O., and Davis, T.N. (2005). A high-efficiency method to replace essential genes with mutant alleles in yeast. Yeast *22*, 769-774.

Yeh, E., Haase, J., Paliulis, L.V., Joglekar, A., Bond, L., Bouck, D., Salmon, E.D., and Bloom, K.S. (2008). Pericentric chromatin is organized into an intramolecular loop in mitosis. Curr Biol *18*, 81-90.

Zitouni, S., Nabais, C., Jana, S.C., Guerrero, A., and Bettencourt-Dias, M. (2014). Polo-like kinases: structural variations lead to multiple functions. Nat Rev Mol Cell Biol *15*, 433-452.

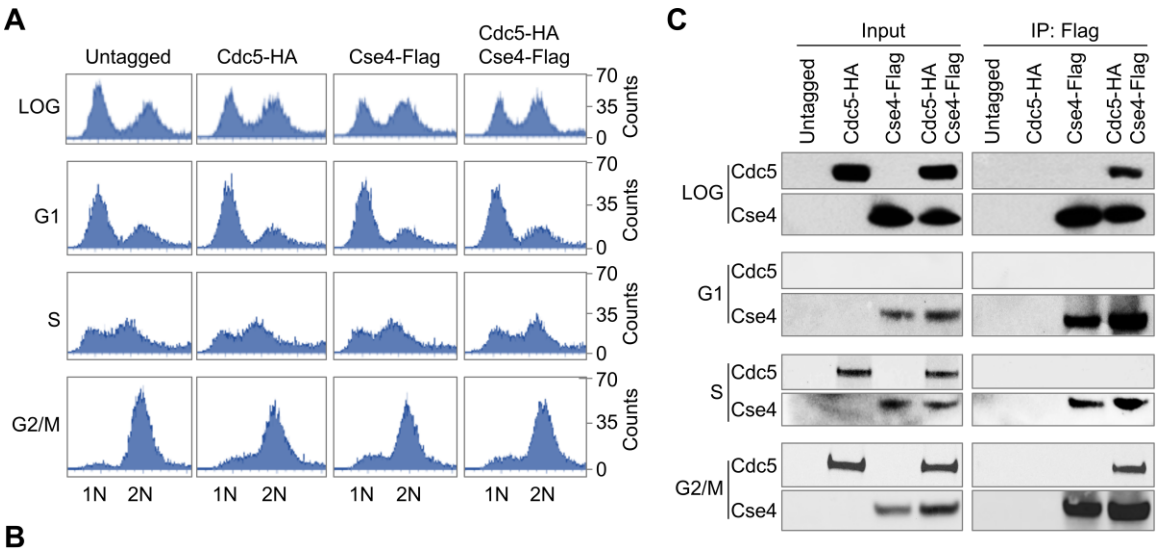

B

G1 S G2/M	Untagged			Cdc5-HA			Cse4-Flag			Cdc5-HA Cse4-Flag		
	G1	S	G2/M	G1	S	G2/M	G1	S	G2/M	G1	S	G2/M
Asynchronous (LOG)	36	14	50	32	12	56	25	22	53	29	10	61
alpha-factor (G1)	87	4	9	91	3	6	93	2	5	86	1	13
HU (S)	9	80	11	7	83	10	3	87	10	7	81	12
Nocodazole (G2/M)	3	5	92	8	6	86	9	2	89	4	2	94

FIGURE 1. Cdc5 interacts *in vivo* with Cse4 in a cell cycle dependent manner. Strains carrying vector control (Untagged, YMB9325), Cdc5-HA (YMB9326), Cse4-Flag (YMB9327), and Cdc5-HA Cse4-Flag (YMB9328) were grown at 30°C to logarithmic phase and synchronized in G1, S and G2/M stages of the cell cycle. Cell extracts were prepared for immunoprecipitation experiments using α-Flag agarose antibodies. (A) FACS profiles show DNA content in different stages of the cell cycle. (B) Cell cycle stages were determined based on nuclear position and cell morphology by microscopic examination of at least 100 cells for each sample. Different stages of the cell cycle: G1, S phase (S), and mitosis (G2/M). (C) *In vivo* interaction of Cdc5 with Cse4 is observed in G2/M cells. Immunoprecipitated proteins were analyzed by Western blotting with α-HA (Cdc5), and α-Flag (Cse4) antibodies. IP-Flag represents immunoprecipitated samples.

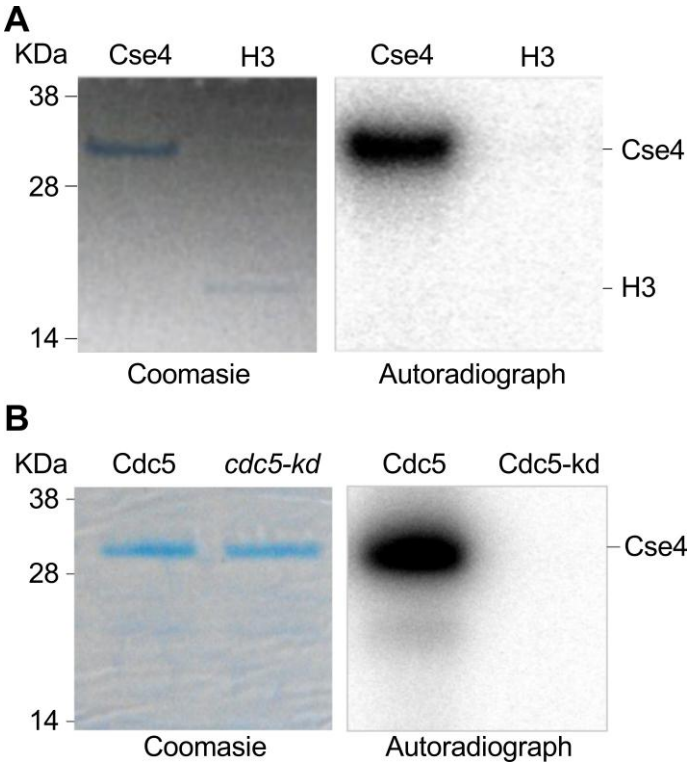

FIGURE 2. Cdc5 phosphorylates Cse4 *in vitro* mediated by its kinase domain. (A) Cdc5 phosphorylates Cse4 *in vitro*. Kinase assays were carried out *in vitro* using purified Cse4, Cdc5 and radiolabeled ATP at 30°C for 60 minutes and products were analyzed by SDS gel electrophoresis followed by Coomassie Blue staining and autoradiography of radiolabeled proteins. Purified histone H3 with Cdc5 served as control. (B) Phosphorylation of Cse4 is mediated by the kinase domain of Cdc5. *In vitro* kinase assays were carried out using purified Cse4, Cdc5 or Cdc5kd [K100M, a kinase-dead variant of Cdc5; (Ratsima *et al.*, 2011)] and radiolabeled ATP as described above.

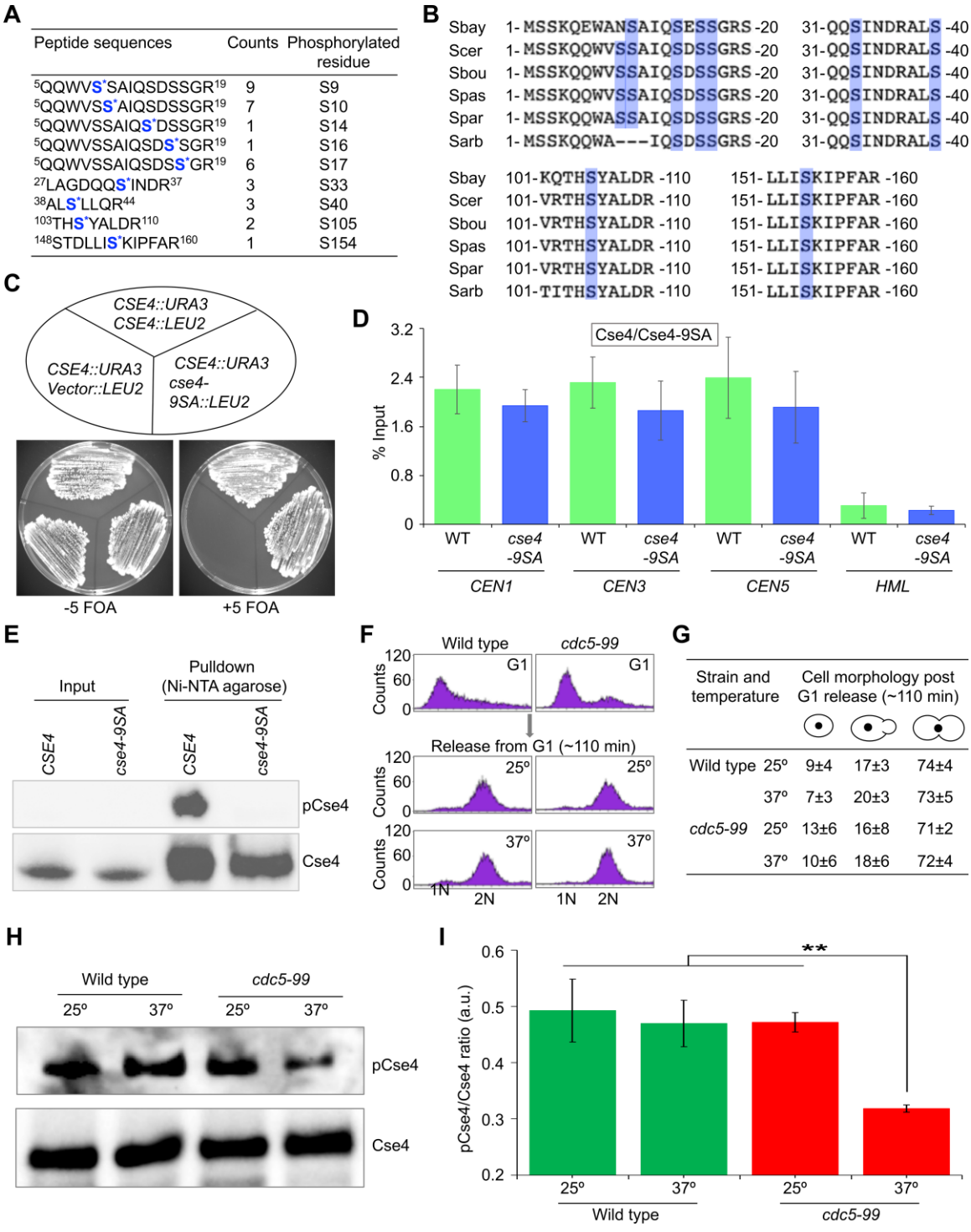

FIGURE 3. Cdc5 phosphorylates Cse4 at its N-terminus *in vitro*, and contributes to Cse4 phosphorylation *in vivo*. (A) Cse4 peptides phosphorylated *in vitro* by Cdc5 were identified by LC-MS/MS. Phosphorylated serines are marked with in blue colored shade.

(B) The region containing the phosphorylated serines within the Cse4 (shaded blue) is evolutionarily conserved among yeasts with point centromeres. ClustalW alignment of the Cse4 regions of: Sbay = *Saccharomyces bayanus*, Scer = *S. cerevisiae*, Sbou = *S. boulardii*, Spas = *S. pastorianus*, Spar = *S. paradoxus*, and Sarb = *S. arboricola*. (C) *cse4-9SA* mutant is viable. Wild type strain with *CSE4::URA3* (pRB199) was transformed with *vector::LEU2* (YMB10341), *CSE4::LEU2* (YMB10049), or *cse4-9SA::LEU2* (YMB10339). Strains were plated on synthetic medium without or with counterselection for *URA3* by 5′-fluorootic acid (5-FOA) and incubated for 7 days at 25°C. (D) The levels of Cse4 and Cse4-9SA are not significantly different at the *CEN* chromatin. Wild type (WT, YMB9383), and *cse4-9SA* (YMB10593) strains were grown in YPD to logarithmic phase at 25°C, and ChIP for endogenously expressed HA-tagged Cse4 or Cse4-9SA was performed using α-HA agarose antibodies. Enrichment of Cse4 or Cse4-9SA at *CEN1*, *CEN3*, *CEN5*, and a negative control (*HML*) was determined by qPCR and is presented as % input. Average from three biological replicates ± standard error is shown. No statistically significant difference was observed between wild type and cse4-9SA strains (*p*-value = 0.05, Student's *t*-test). (E) Cse4-9SA protein does not react with αp-Cse4 antibodies. Wild type strains transformed with *GAL1-6HIS-3HA-CSE4* (YMB10426) or *GAL1-6HIS-3HA-cse4-9SA* (YMB10427) were grown to logarithmic phase of growth in synthetic medium, and gene expression was induced in the presence of galactose plus raffinose (2% each) at 25°C for about four generations of growth. Protein extracts were prepared for affinity purification of Cse4 or Cse4-9SA strains using Ni^{2+}-NTA agarose. Eluted proteins were analyzed by Western blotting. Antibodies used were α-HA (Cse4) and αp-Cse4 specific (pCse4) antibodies (Boeckmann *et al.*, 2013).

(F) Cdc5 contributes to Cse4 phosphorylation *in vivo*. FACS profiles show G1 synchronization, and release into pheromone free media to enrich cells in metaphase. Wild type (YMB10986) and *cdc5-99* (YMB10987) strains expressing *GAL1-6HIS-3HA-CSE4* (pMB1601) were synchronized in G1 (1.5 μM α-factor) in 1x SC-URA galactose plus raffinose (2% each) for 2 hours at 25°C. Cells were collected, washed with water, and released into pheromone free 1x SC-URA galactose plus raffinose (2% each) at 25° and 37°C for ~110 min (~ 70% cells in metaphase). Proteins extracts were prepared, and affinity purified as described in (E). (G) Cell and nuclear morphology of strains from (F) post-G1 release into pheromone free media (~110 min) showing enrichment of cells in metaphase stage of the cell cycle. Average from three biological replicates ± standard deviation is shown. (H) Western blotting show reduction of Cse4 phosphorylation in *cdc5-99* at non-permissive temperature of 37°C. Affinity-purified proteins from strains grown in (E) were separated on polyacrylamide gels, and transferred to nitrocellulose membranes. Blots were probed with antibodies: α-HA (total Cse4), and αp-Cse4 antibodies (Boeckmann *et al.*, 2013). Three biological replicates were performed. (I) Quantification of relative phosphorylation of Cse4 from Western blots. Ratio of phosphorylated Cse4 (pCse4) to the total Cse4 levels (Cse4) in wild type and *cdc5-99* strains was calculated. The histogram represents the average of three biological replicates ± standard error. **$p < 0.01$, Student's t test.

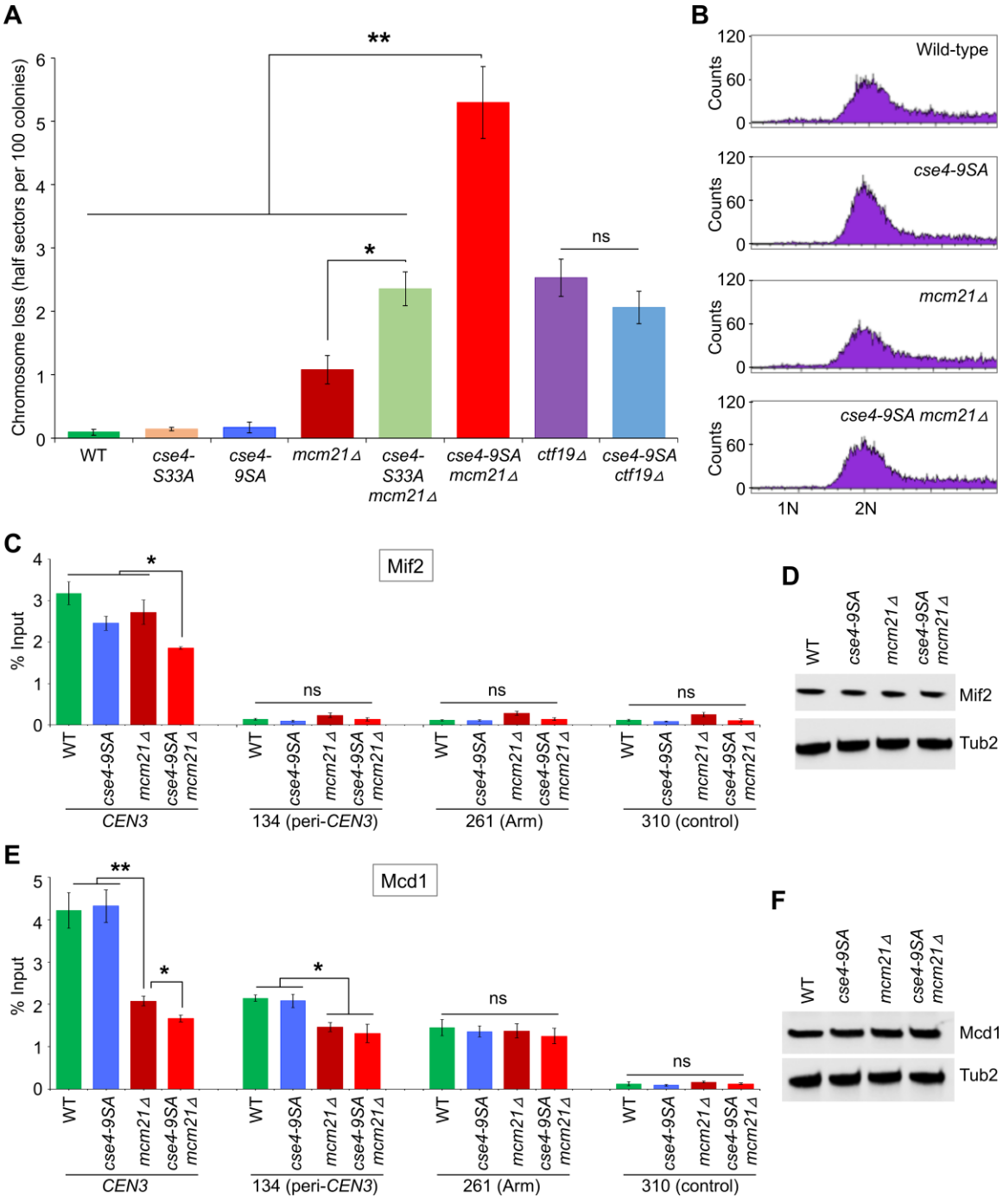

FIGURE 4. Cdc5 mediated phosphorylation contributes to faithful chromosome segregation and modulates the levels of Mif2 and Mcd1/Scc1 at the *CEN* chromatin. (A) Errors in chromosome segregation are increased in *cse4-9SA mcm21Δ* strains. Frequency of CF loss in wild type (YPH1018), *cse4-S33A* (YMB10984), *cse4-9SA* (YMB10337),

mcm21Δ (YMB10645), *cse4-S33A mcm21Δ* (YMB10985), *cse4-9SA mcm21Δ* (YMB10646), *ctf19Δ* (YMB10647), and *cse4-9SA ctf19Δ* (YMB10648) strains was determined using a colony color assay as described in materials and methods. At least 1000 colonies from three independent transformants were counted and average from three biological experiments ± standard error is shown. ***p*-value <0.01, ns = statistically not significant, Student's *t*-test. (B) The *CEN* levels of Mif2 and Mcd1/Scc1 are reduced in *cse4-9SA mcm21Δ* strains. FACS profiles show DNA content representing G2/M stage of the cell cycle. Wild type (YMB9695), *cse4-9SA* (YMB10593), *mcm21Δ* (YMB10740), and *cse4-9SA mcm21Δ* (YMB10741) carrying Mcd1-GFP were grown in YPD to logarithmic phase at 30°C, and synchronized in G2/M with nocodazole. ChIP was performed using α-Mif2 antibodies and α-GFP sepharose beads (Mcd1/Scc1) as described in materials and methods. (C) Enrichment of Mif2 at *CEN3*, *CAR* (134, and 261) and non-*CAR* control region (310) on chromosome III was determined by ChIP-qPCR and is presented as % input. Average values from three biological replicates ± standard error is shown. **p*-value <0.05, ns = statistically not significant, Student's *t*-test. (D) Western blotting showing expression of Mif2 in strains used in ChIP experiments. Antibodies used were: α-Mif2, and α-Tub2 (loading control). (E) Enrichment of Mcd1/Scc1 at *CEN3*, *CAR* (134, and 261) and non-*CAR* control region (310) on chromosome III was determined by ChIP-qPCR and is presented as % input. Average values from three biological replicates ± standard error is shown. ***p*-value <0.01, **p*-value <0.05, ns = statistically not significant, Student's *t*-test. (F) Western blotting showing expression of Mcd1/Scc1 in strains used in ChIP experiments. Antibodies used were: α-GFP, and α-Tub2 (loading control).

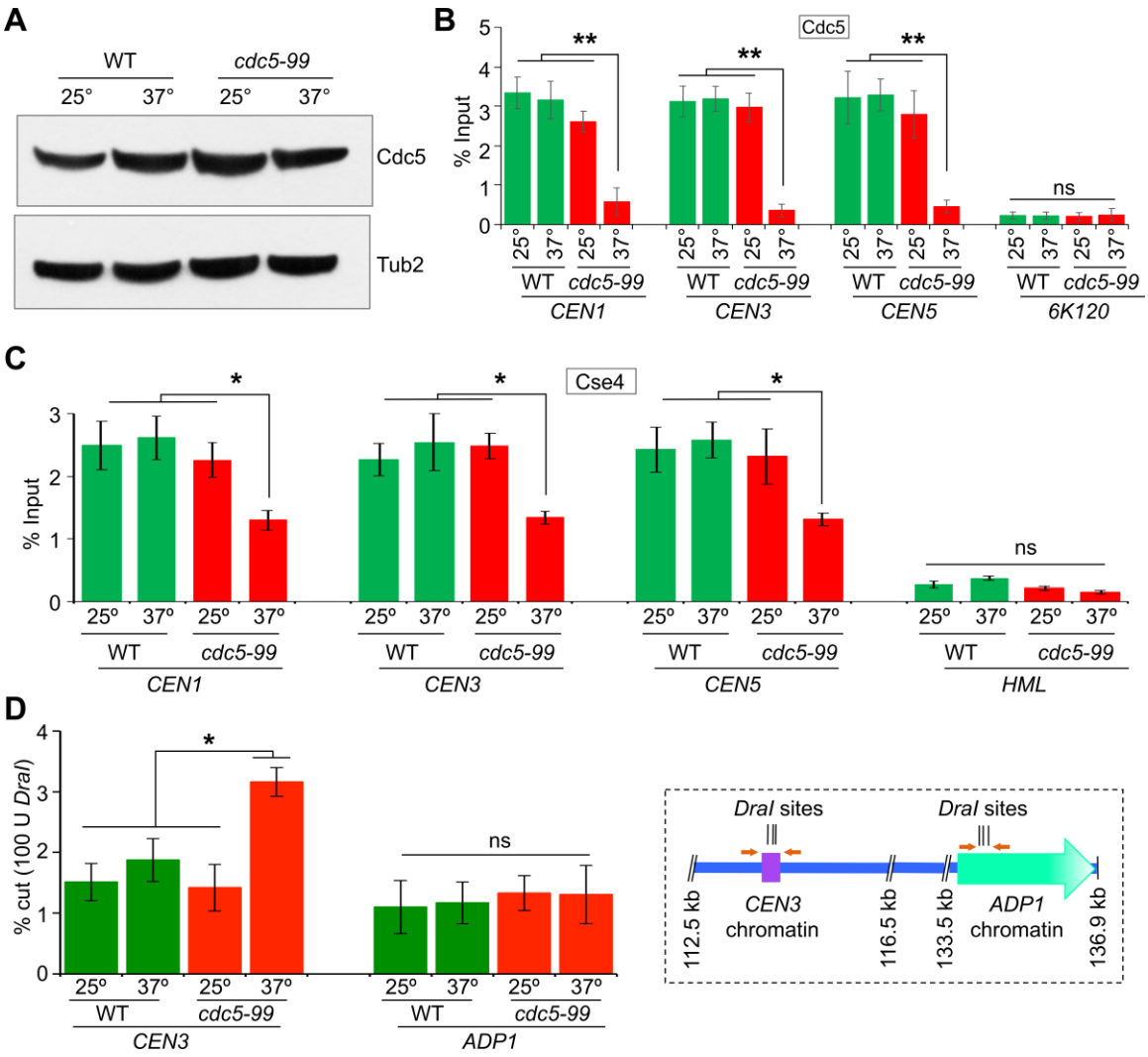

FIGURE 5. Loss of Cdc5 from *CEN* correlates with the reduction in *CEN* associated Cse4 and defects in structural integrity of kinetochores. (A) Expression of Cdc5 is not affected in *cdc5-99* mutant grown at the non-permissive temperature (37°C). Wild type (YMB9431), and *cdc5-99* (YMB9432) were grown to logarithmic phase at 25°C, and shifted to non-permissive temperature (37°C) for 2.5 hours. Whole cell extracts were prepared, and Western blots were done using α-Cdc5 and α-Tub2 (loading control) antibodies. (B) Cdc5-99 does not associate with *CEN* at the non-permissive temperature (37°C) in *cdc5-99* strain. ChIP was performed in strains as described in (A) using α-

Cdc5 antibodies. Enrichment of Cdc5 at *CEN1*, *CEN3*, *CEN5* and a negative control (6K120) was determined by qPCR and is presented as % input. Average from three biological replicates ± standard error is shown. ***p*-value <0.01, ns = statistically not significant, Student's *t*-test. (C) Cdc5 regulates the levels of Cse4 at the *CEN*. Wild type (YMB9383), and *cdc5-99* (YMB9175) were grown in YPD to logarithmic phase at 25°C, and shifted to non-permissive temperature (37°C) for 6 hours. ChIP for HA-tagged Cse4 was performed using α-HA agarose antibodies. Enrichment of Cse4 at *CEN1*, *CEN3*, *CEN5*, and a negative control (*HML*) was determined by qPCR and is presented as % input. Average from three biological replicates ± standard error is shown. **p*-value <0.05, ns = statistically not significant, Student's *t*-test. (D) Cdc5 is required for the structural integrity of kinetochores. Wild type (KBY2012), and *cdc5-99* (YMB9367) were grown in YPD to logarithmic phase at 25°C, and shifted to non-permissive temperature (37°C) for 6 hours. Nuclei were extracted and incubated with 100 Units of *DraI* restriction endonuclease at 37°C for 30 min as described in Materials and Methods. *DraI* accessibility at *CEN3* and *ADP1* (control) chromatin is shown. Average from three biological experiments ± standard error is shown. **p*-value <0.05, ns = statistically not significant, Student's *t*-test. Right insert: schematic modified from our previous study (Mishra *et al.*, 2013) for *CEN3* and *ADP1* regions examined for *DraI* accessibility.

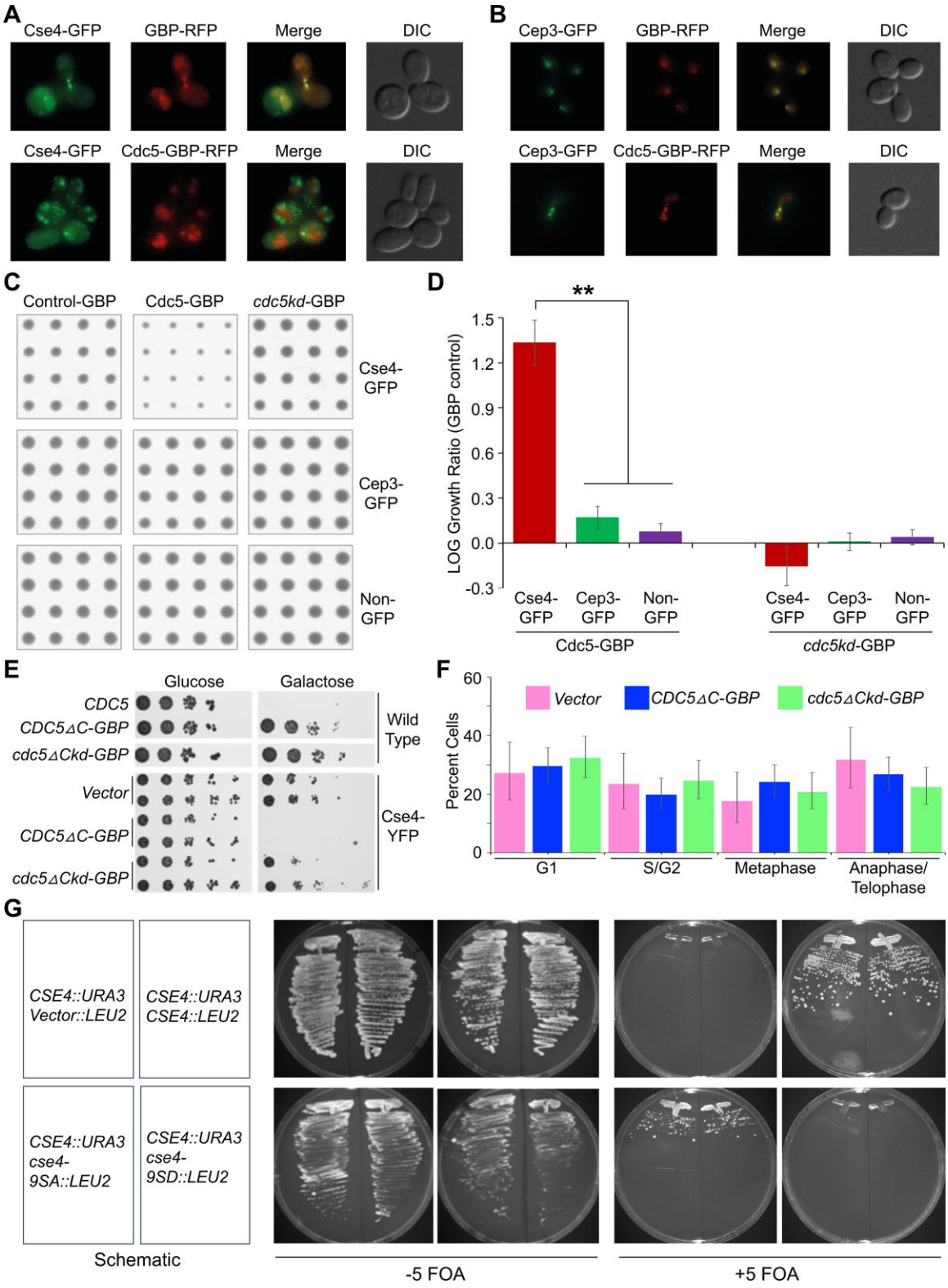

FIGURE 6. Cell cycle regulated interaction of Cdc5 with Cse4 is required for cell growth. A Synthetic Physical Interaction (SPI) assay was performed using plasmids

expressing Cdc5-GBP, *cdc5kd*-GBP (kinase dead version) or GBP alone, which were introduced into Cse4-GFP (internally tagged), Cep3-GFP and non-GFP strains. (A) The cells from the SPI screen were grown overnight in 1x SC-Leu +Ade with 2% galactose medium at 23˚C and imaged using fluorescence microscopy. The GBP-RFP and Cdc5-GBP-RFP signal colocalizes with the GFP signal. Cells with Cse4-GFP and Cdc5-GBP-RFP show multiple Cse4-GFP foci in contrast to Cse4-GFP cells containing GBP-RFP control. (B) Cep3-GFP cells containing either Cdc5-GBP-RFP or GBP-RFP control show normal kinetochore foci, each image is 20.6 µm square. (C) Representative images of the scanned plates from the SPI screen show 16 replicates for each strain (rows) and plasmid (columns) combination. (D) The colony sizes in (C) were measured and log growth ratios plotted for the GFP and wild-type strains with *pCUP1-GBP* as controls for each comparison. Error bars indicate standard deviation from the mean. ***p*-value <0.01, Student's *t*-test. (E) The forced association of Cdc5 with Cse4 does not arrest cells at a specific cell cycle stage. Ten-fold serial dilutions of wild-type and *CSE4-YFP* (T664) strains carrying the *GAL1-CDC5* (pHT573), *GAL1-CDC5*Δ*C-GBP* (pHT580), *GAL1-cdc5kd*Δ*C-GBP* (pHT581), and *GAL1-Vector* (pHT103) plasmids were spotted onto 1x SC-Leu media containing either 2% glucose (expression OFF) or 2% galactose (expression ON), and grown at 30˚C for two days. (F) Quantification of the cell cycle stages of the *CSE4-YFP* (T664) strain carrying either the *GAL1-Cdc5*Δ*C-GBP* or the *GAL1-Vector* and *GAL1-cdc5kd*Δ*C-GBP* control plasmids after growing to logarithmic phase in 1x SC-Leu 2% raffinose media, and then swapped to 1x SC-Leu 2% galactose media for four hours. The cell cycle stage was assessed by fluorescence microscopy, each cell was counted and given the following cell cycle category: non-budded cells were

categorized as G1 cells, small-budded as S/G2, large-budded cells with two Cse4-YFP foci in the bud neck as Metaphase (M), and large-budded cells with completely separated Cse4-YFP foci in the mother and daughter as anaphase/telophase cells. No statistical difference was found between Cdc5ΔC-GBP to either control as evaluated by Fisher's exact test. Error bars indicate 95% confidence interval. (G) *cse4-9SD* mutant is unable to complement the growth defect of *cse4*Δ strain. Wild type strain with *CSE4::URA3* (pRB199) was transformed with *vector::LEU2* (YMB10341), *CSE4::LEU2* (YMB10049), *cse4-9SA::LEU2* (YMB10339), or *cse4-9SD::LEU2* (YMB10340). Strains were streaked on synthetic medium without or with counterselection for *URA3* by 5′-fluorootic acid (5-FOA) and incubated for 6 days at 25°C.

TABLE 1. List of strains, and plasmids used in this study.

(A) *Saccharomyces cerevisiae* strains:		
Strain	Genotype	Reference
YMB9325	*MATa ura3-52 lys2-801 ade2-101 trp1Δ63 his3Δ200 leu2Δ1 TRP1::CEN URA3::CEN*	This study
YMB9326	*MATa ura3-52 lys2-801 ade2-101 trp1Δ63 his3Δ200 leu2Δ1 CDC5-3HA::TRP1 URA3::CEN*	This study
YMB9327	*MATa ura3-52 lys2-801 ade2-101 trp1Δ63 his3Δ200 leu2Δ1 TRP1::CEN GAL1-FLAG-CSE4::URA3*	This study
YMB9328	*MATa ura3-52 lys2-801 ade2-101 trp1Δ63 his3Δ200 leu2Δ1 CDC5-3HA::TRP1 GAL1-FLAG-CSE4::URA3*	This study
YMB10341	*MATα cse4Δ::kanMX pRS416-CSE4 (pRB199) GAL1-Vector::LEU2*	TianYi Zhang
YMB10049	*MATα cse4Δ::kanMX pRS416-CSE4 (pRB199) GAL1CSE4-3HA::LEU2*	TianYi Zhang
YMB10339	*MATα cse4Δ::kanMX pRS416-CSE4 (pRB199) GAL1cse4-9SA-3HA::LEU2*	This study
YMB10340	*MATα cse4Δ::kanMX pRS416-CSE4 (pRB199) GAL1cse4-9SD-3HA::LEU2*	This study
YPH1018	*MATα ura3-52 lys2-801 ade2-101 trp1Δ63 his3Δ200 leu2Δ1 CFIII (CEN3L.YPH278) HIS3 SUP11*	Phil Hieter
YMB10337	*MATα ura3-52 lys2-801 ade2-101 trp1Δ63 his3Δ200 leu2Δ1 CFIII (CEN3L.YPH278) HIS3 SUP11 cse4-9SA-3HA::URA3*	This study
YMB10645	*MATα ura3-52 lys2-801 ade2-101 trp1Δ63 his3Δ200 leu2Δ1 CFIII (CEN3L.YPH278) HIS3 SUP11 mcm21Δ::kanMX*	This study
YMB10646	*MATα ura3-52 lys2-801 ade2-101 trp1Δ63 his3Δ200 leu2Δ1 CFIII (CEN3L.YPH278) HIS3 SUP11 mcm21Δ::kanMX cse4-9SA-3HA::URA3*	This study
YMB10647	*MATα ura3-52 lys2-801 ade2-101 trp1Δ63 his3Δ200 leu2Δ1 CFIII (CEN3L.YPH278) HIS3 SUP11 ctf19Δ::kanMX*	This study
YMB10648	*MATα ura3-52 lys2-801 ade2-101 trp1Δ63 his3Δ200 leu2Δ1 CFIII (CEN3L.YPH278) HIS3 SUP11 ctf19Δ::kanMX cse4-9SA-3HA::URA3*	This study
YMB10984	*MATα ura3-52 lys2-801 ade2-101 trp1Δ63 his3Δ200 leu2Δ1 CFIII (CEN3L.YPH278) HIS3 SUP11 cse4-S33A-3HA::NAT*	This study
YMB10985	*MATα ura3-52 lys2-801 ade2-101 trp1Δ63 his3Δ200 leu2Δ1 CFIII (CEN3L.YPH278) HIS3*	This study

	SUP11 mcm21Δ::kanMX cse4-S33A-3HA::NAT	
YMB9695	*MATa MCD1-GFP leu2-3112 ura3-52 his3-11,15 bar1 GAL+ SPC29-RFP::Hyg*	(Mishra *et al.*, 2016)
YMB10593	*MATa MCD1-GFP leu2-3112 ura3-52 his3-11,15 bar1 GAL+ SPC29-RFP::Hyg cse4-9SA-3HA::URA3*	This study
YMB10740	*MATa MCD1-GFP leu2-3112 ura3-52 his3-11,15 bar1 GAL+ SPC29-RFP::Hyg mcm21Δ::HIS3*	This study
YMB10741	*MATa MCD1-GFP leu2-3112 ura3-52 his3-11,15 bar1 GAL+ SPC29-RFP::Hyg mcm21Δ::HIS3 cse4-9SA-3HA::URA3*	This study
YMB9431	*MATα ura3-1 leu2-3112 his3-11,15 trp1-1 ade2-1 can1-100 Smc3-GFP::URA3*	This study
YMB9432	*MATα ura3-1 leu2-3112 his3-11,15 trp1-1 ade2-1 can1-100 Smc3-GFP::URA3 cdc5-99::HIS3MX*	This study
YMB9383	*MATa ade2-1 ura3-1 his3-11,15 trp1-1 leu2,3–112 can1-100 CSE4-3HA::NAT*	This study
YMB9175	*MATa ade2-1 ura3-1 his3-11,15 trp1-1 leu2,3–112 can1-100 CSE4-3HA::NAT cdc5-99::HIS3MX*	This study
KBY2012	*MATa trp1Δ63 leu2Δ ura3-52 his3 Δ 200 lys2-8Δ1 CSE4GFP::TRP1 (pKK1) SPC29CFP::kanMX*	(Haase *et al.*, 2013)
YMB9367	*MATa trp1Δ63 leu2Δ ura3-52 his3 Δ 200 lys2-8Δ1 CSE4GFP::TRP1 (pKK1) SPC29CFP::kanMX cdc5-99::HIS3MX*	This study
W8164-2B	*MATα CEN1-16::Gal-Kl-URA3*	(Reid *et al.*, 2011)
CEP3-GFP strain	*MATa his3Δ1 leu2Δ0 met15Δ0 ura3Δ0 CEP3-GFP::HIS3*	(Huh *et al.*, 2003)
T548	*MATa his3Δ1 leu2Δ0 met15Δ0 ura3Δ0 CSE4-GFP (internal)::HIS3MX6*	This study
BY4742	*MATα his3Δ1 leu2Δ0 met15Δ0 ura3Δ0*	Resgen Inc.
T664	*MATα his3Δ1 leu2Δ0 lys2Δ0 ura3Δ0 CSE4-YFP (internal)::HIS3MX6*	This study
YMB10426	*MATa ura3-1 leu2-3112 his3-11,15 trp1-1 ade2-1 can1-100 GAL1-6HIS-3HA-CSE4::LEU2* (pMB1515)	This study
YMB10427	*MATa ura3-1 leu2-3112 his3-11,15 trp1-1 ade2-1 can1-100 GAL1-6HIS-3HA-cse4-9SA::LEU2* (pMB1847)	This study
YMB10986	*MATa ade2-1 ura3-1 his3-11,15 trp1-1 leu2,3-112 can1-100 GAL1-6HIS-3HA-CSE4::URA3* (pMB1601)	This study
YMB10987	*MATa ade2-1 ura3-1 his3-11,15 trp1-1 leu2,3-112 can1-100 cdc5-99::HIS3MX6 GAL1-6HIS-3HA-CSE4::URA3* (pMB1601)	This study
(B) List of plasmids:		

Plasmid	Description	Reference
p344	*CDC5-3HA::TRP1*	D. D'Amours
pRB199	*CSE4-3HA::URA3*	R.Baker
pHT4	*pCUP1-GBP-RFP LEU2*	(Olafsson and Thorpe, 2015)
pHT425	*pCUP- CDC5-GBP LEU2*	This study
pHT442	*pCUP1-cdc5kd-GBP LEU2*	This study
pHT103	*pGAL1-empty LEU2*	(Olafsson and Thorpe, 2016)
pHT573	*pGAL1-CDC5 LEU2*	This study
pHT580	*pGAL1-CDC5ΔC-GBP LEU2*	This study
pHT581	*pGAL1-cdc5kdΔC-GBP LEU2*	This study
pMB1515	*pGAL1-6HIS-3HA-CSE4 LEU2*	This study
pMB1847	*pGAL1-6HIS-3HA-cse4-9SA LEU2*	This study
pMB1601	*pGAL1-6HIS-3HA-CSE4 URA3*	This study

TABLE 2. List of primers used in this study.

Locus	Forward (5' - 3')	Reverse (5' - 3')	Reference
CEN1	CTCGATTTGCATAAGTGTGCC	GTGCTTAAGAGTTCTGTACCAC	(Choy *et al.*, 2011)
CEN3	GATCAGCGCCAAACAATATGG	AACTTCCACCAGTAAACGTTTC	(Choy *et al.*, 2011)
CEN5	AAGAACTATGAATCTGTAAATGACTGATTCAAT	CTTGCACTAAACAAGACTTTATACTACGTTTAG	(Choy *et al.*, 2011)
6K120	AACGTCACTTTTTTTCCAGGG	GCAAAGCTAGCTAACGAACAA	(Mishra *et al.*, 2016)
HML	CACAGCGGTTTCAAAAAAGCTG	GGATTTTATTTAAAAATCGAGAGG	(Choy *et al.*, 2011)
CEN3-DraI	TTGATGAACTTTTCAAAGATGAC	GTCAACGAGTCCTCTCTGGCTA	(Choy *et al.*, 2011)
ADP1	ATCCAAATGTGCTCAAGATAGTAGC	CACCAAACAACATTTACTAGCAGTG	(Mishra *et al.*, 2013)
134	CCGATGGTTAGGATTTCCAACG	GGTTTTCAGAACAGAATGGGGC	(Eckert *et al.*, 2007; Ng *et al.*, 2009)
261	TTGCCACAGCCACAGATATAACTG	GATGGACAAAGCGTTGTATCCG	(Eckert *et al.*, 2007; Ng *et al.*, 2009)
310	TCTCGGAATTTATCATGACCCAT	AAACCCTGCACACATTTCGT	(Laloraya *et al.*, 2000)